Additive Schwarz Methods for p-and hp-Finite Elements

Joachim Schöberl

A. Bećirović, R. Gaisbauer, S. Zaglmayr

FWF Start Project Y-192
"3D hp-Finite Elements: Fast Solvers and Adaptivity"
RICAM, Austrian Academy of Sciences

V. Pillwein

SFB013 "Numerical and Symbolic Scientific Computing"
Sub-Project "Hypergeometric Summation for High Order FEM"
Johannes Kepler University Linz, Austria

Markus Wabro

FEMworks - Finite Element Software and Consulting GmbH

DD 16, New York, Jan 12-15, 2005

Contents:

1. High Order Finite Elements
2. Schwarz methods for p-version triangles and tetrahedra
3. Anisotropic mesh refinement for edge and corner singularities
4. High order elements for $H(\mathrm{curl})$
5. Spectral FEM on tetrahedra

High Order Finite Elements

- We are interested in variational boundary value problems posed in H^1 and $H(\mathrm{curl})$.
- The high order finite element space is defined on a mesh consisting of (possibly curved) tetrahedral, prismatic, pyramidal and hexahedral elements.

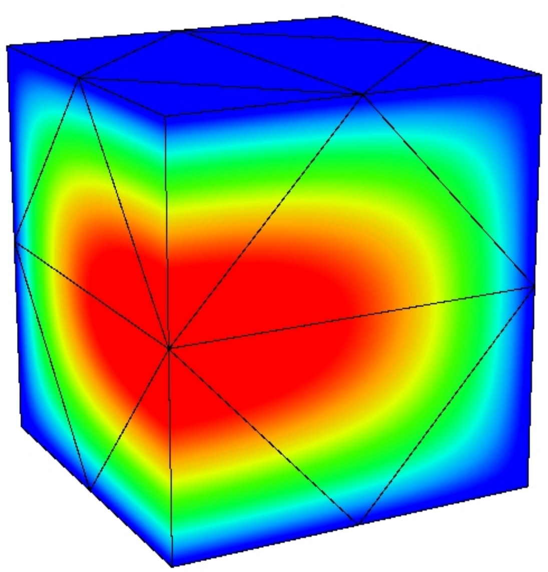

Unstructured tet mesh, $p = 5$

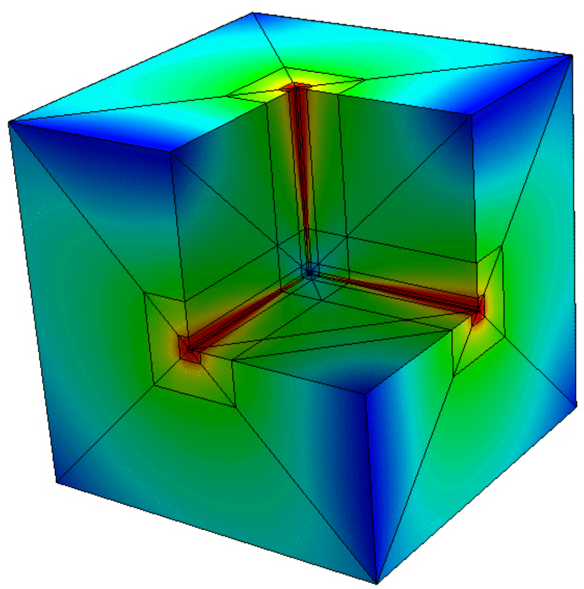

Babuška-type hp-refinement

Stresses in a Wrench (linear elasticity)

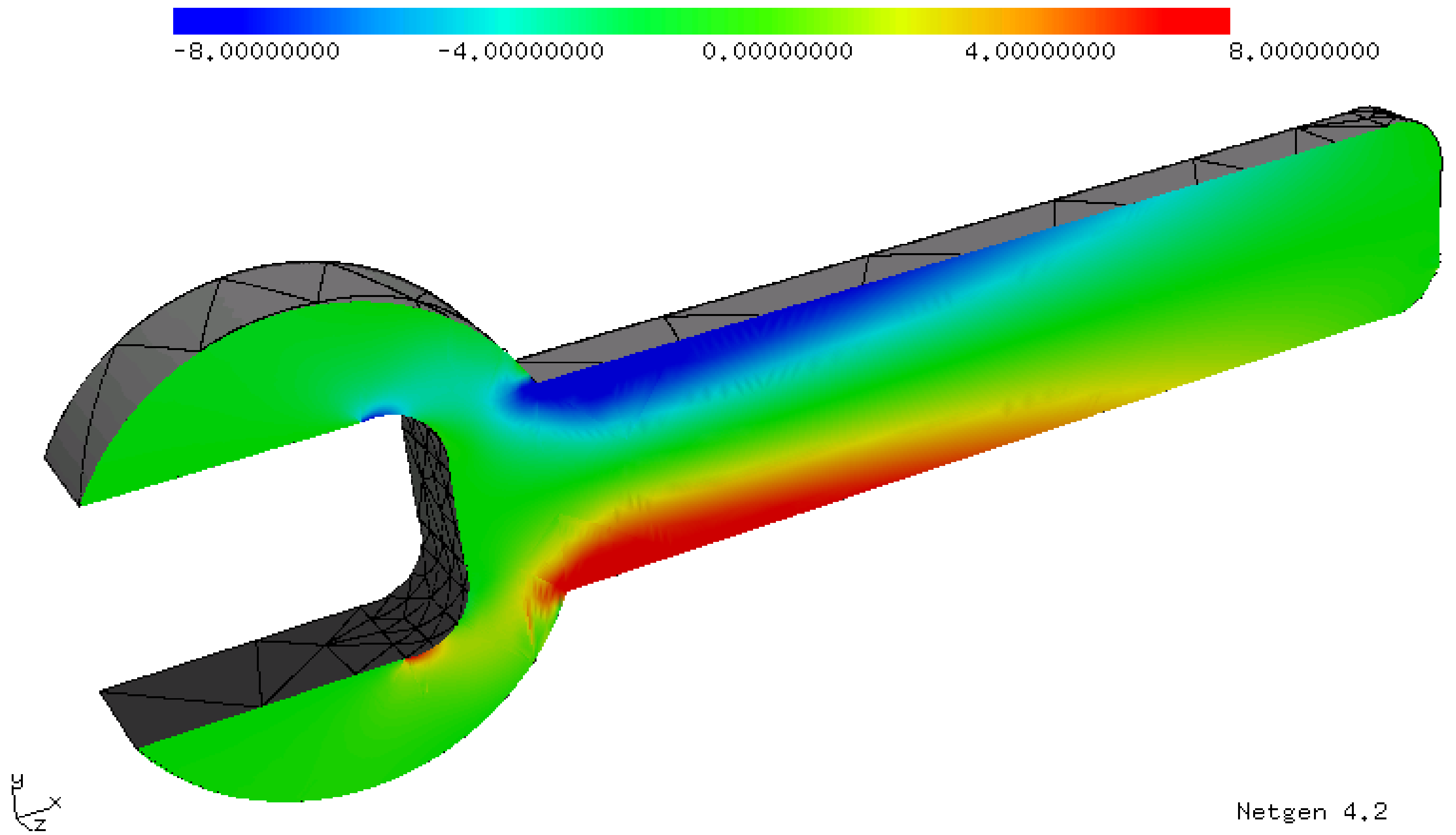

Simulation with Netgen/NGSolve

539 tets, $p = 7$, 108 681 unknowns, 58 PCG-its, 115 sec solver on P-Centrino, 1.7 GHz

Von-Mises Stresses in a Crank-shaft (linear elasticity)

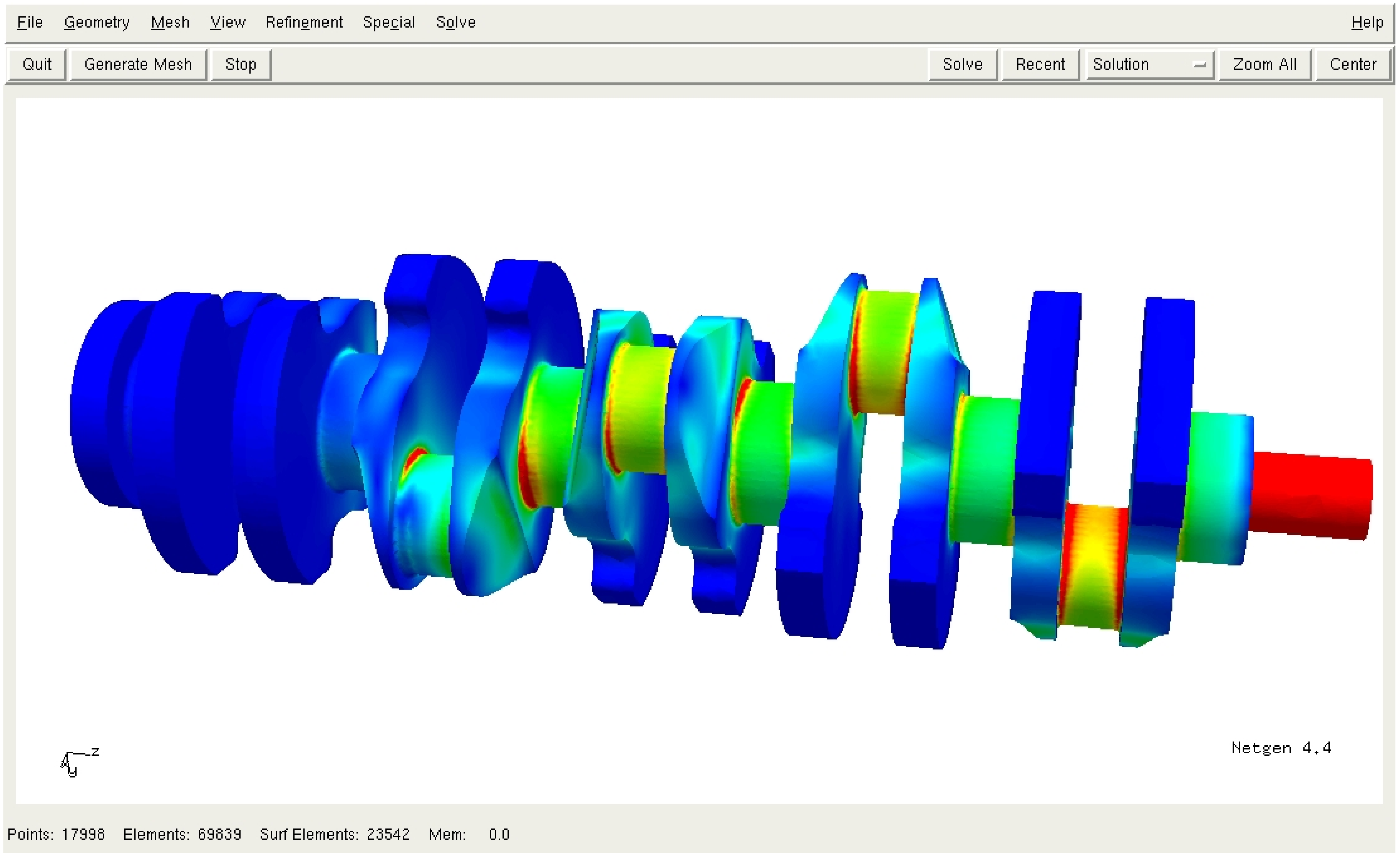

Simulation with Netgen/NGSolve

69839 tets, p = 3, 3×368661 unknowns, 34 min on 2.4 GHz PC 1.2 GB RAM

Thin Structures and High Order Finite Elements

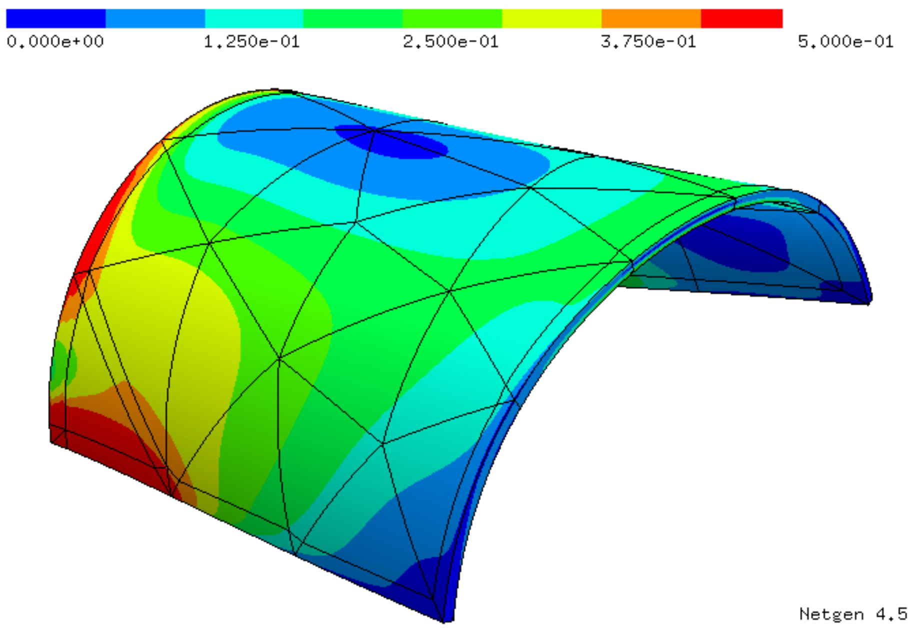

Tensor product elements, $p = 6$

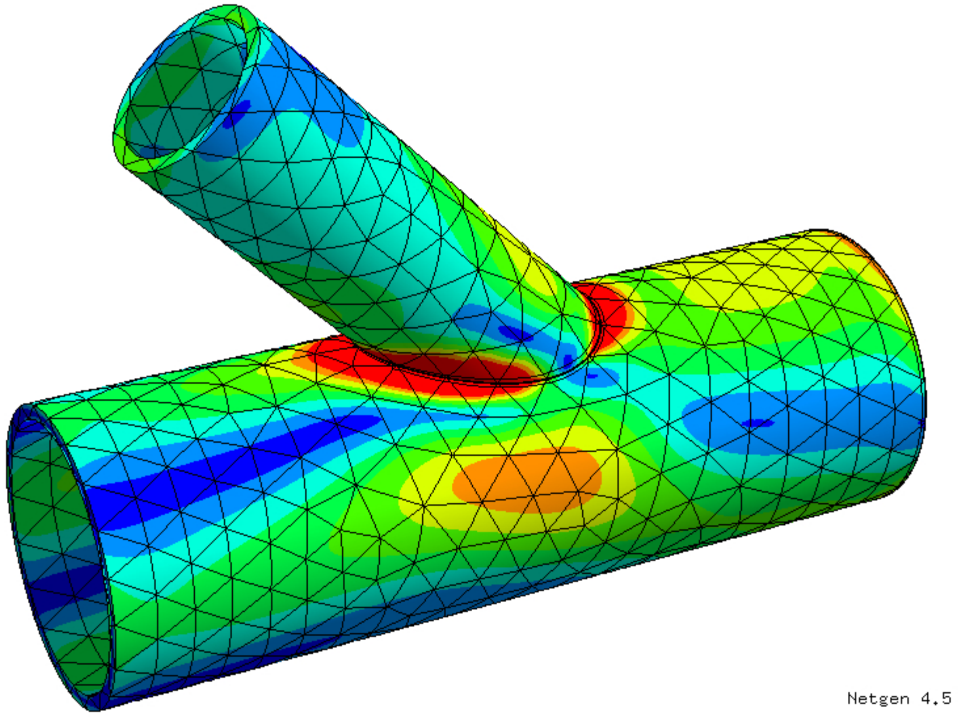

Unstructured tet mesh with anisotropic geometric refinement, $p = 4$

Magnetic field induced by a coil

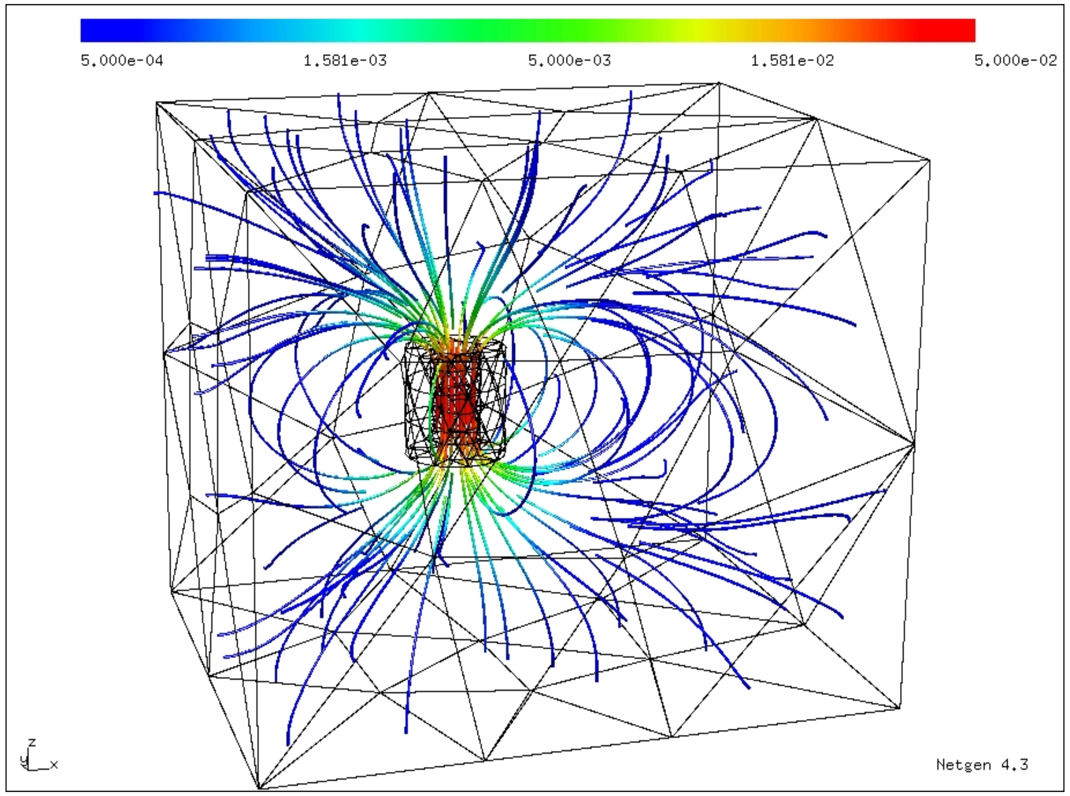

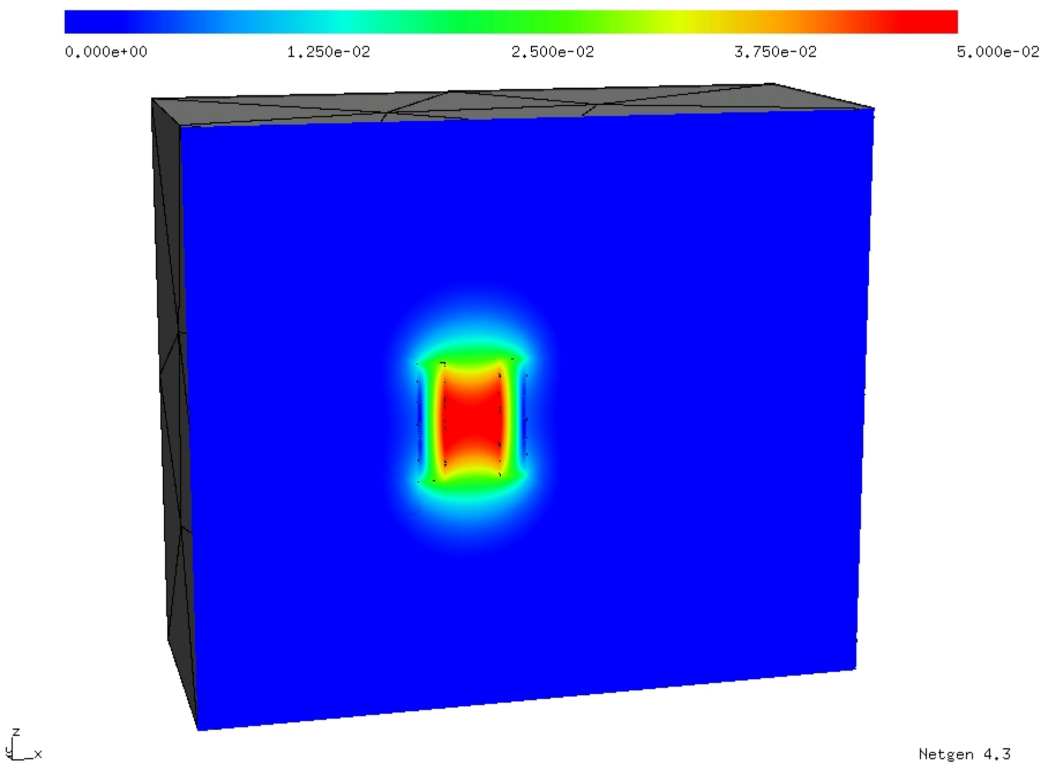

Simulation with Netgen/NGSolve

2035 Nédélec-II tets, $p = 6$, 186 470 unknowns, 59 PCG-its, 87 sec solver time

Hierarchic $V - E - F - I$ basis for H^1-conforming Finite Elements

The high order elements have basis functions connected with the vertices, edges, (faces,) and elements of the mesh:

Vertex basis function

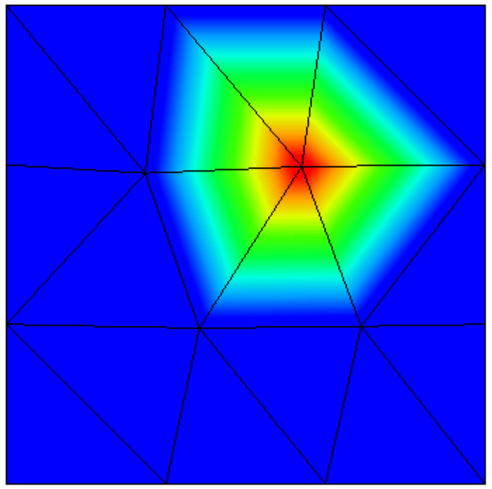

Edge basis function p=3

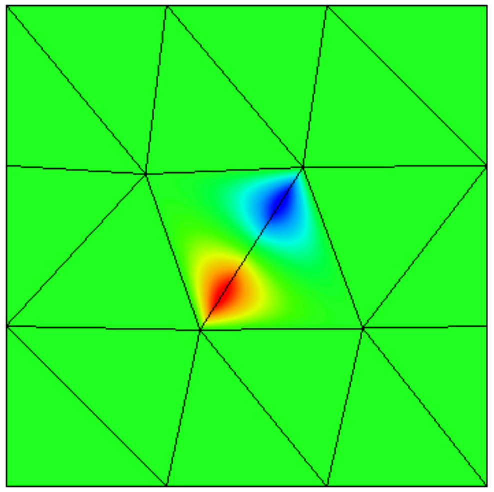

Inner basis function p=3

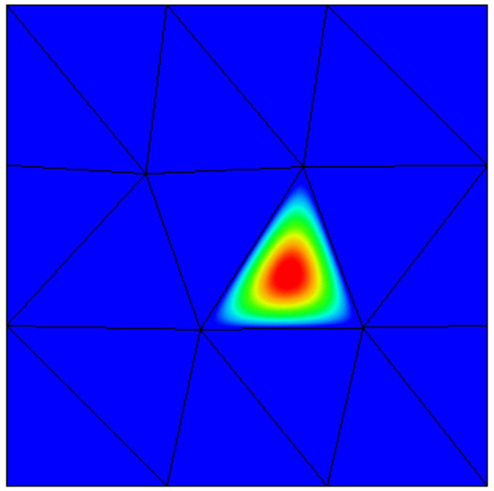

This allows an individual order for each edge, face, and element.

Construction of high order finite elements in 1D

Usually, one chooses $hierarchic$ shape functions on the reference element $(-1, 1)$:

$$\varphi_0(x) = \frac{1+x}{2} \qquad \varphi_1(x) = \frac{1-x}{2} \qquad \varphi_i = (1-x^2)\psi_{i-2} \text{ with } \psi_{i-2} \in P^{i-2}(-1,1)$$

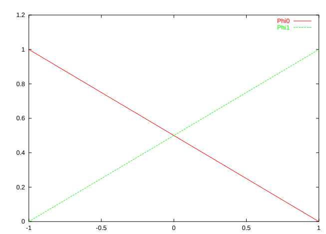

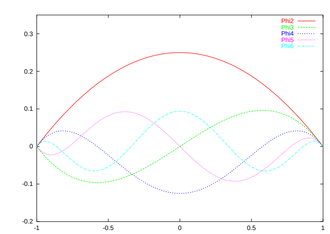

Most often, ψ_i are orthogonal polynomials such as

- Legendre $P(s)$, orthogonal w.r.t. $(p, q) = \int_{-1}^{+1} p(x)q(x)dx$,
- Gegenbauer $C^\lambda(s)$, orthogonal w.r.t. $(p, q) = \int_{-1}^{+1} (1-x^2)^{\lambda-1/2} p(x)q(x)dx$,
- Jacobi $P^{\alpha,\beta}(s)$, orthogonal w.r.t. $(p, q) = \int_{-1}^{+1} (1+x)^\alpha (1-x)^\beta p(x)q(x)\,dx$

All of them are efficiently computable by 3 term recurrences.

Higher-order H^1-conforming shape functions in tensor product structure

Exploit the tensor product structure of quadrilateral elements to build edge and face shapes

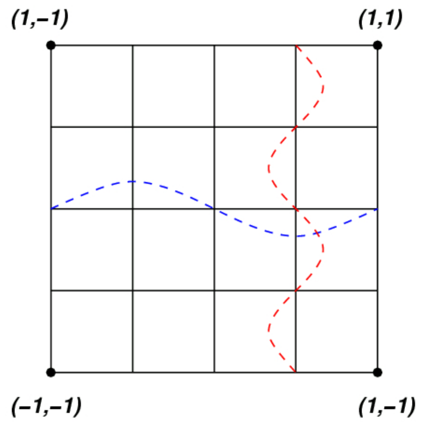

Family of orthogonal polynomials $(\, P_k^0[-1,1]\,)_{2 \leq k \leq p}$ vanishing in ± 1.

$$\begin{aligned}\varphi^F_{i\,j}(x,y) &= P_i^0(x)\, P_j^0(y),\\ \varphi^{E_1}_i(x,y) &= P_i^0(x)\, \tfrac{1-y}{2}.\end{aligned}$$

Tensor-product structure for triangle [Dubiner, Karniadakis+Sherwin]:

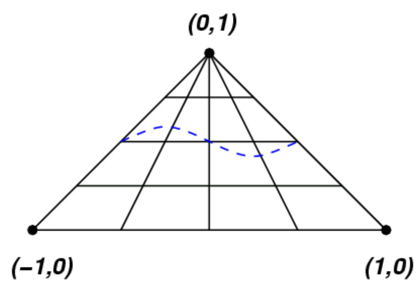

Collapse the quadrilateral to the triangle by $x \to (1-y)x$

$$\begin{aligned}\varphi^{E_1}_i(x,y) &= P_i^0(\tfrac{x}{1-y})\,(1-y)^i\\ \varphi^F_{i\,j}(x,y) &= \underbrace{P_i^0(\frac{x}{1-y})(1-y)^i}_{u_i(x,y)}\ \underbrace{P_j(2y-1)y}_{v_j(y)}\end{aligned}$$

Other edge basis functions by permutation of vertices

Overlapping Schwarz methods for simplicial elements

Let $\mathcal{T}$, $\mathcal{F}$, $\mathcal{E}$, $\mathcal{V}$ be the sets of tetrahedra, faces, edges and vertices. Let ω_F, ω_E, ω_V be the patches of elements sharing the face F, the edge E, and the vertex V, respectively.

Let $V = \{v \in H^1 : v = 0 \text{ on } \Gamma_D\}$, and

$$V_p = \{v \in V : v|_T \in P^p \; \forall T \in \mathcal{T}\}$$

Define the coarse space

$$V_0 = \{v \in V : v|_T \in P^1 \; \forall T \in \mathcal{T}\}$$

and lcoal overlapping vertex-based spaces

$$V_V = \{v \in V_p : v = 0 \text{ in } \Omega \setminus \omega_V\}$$

Theorem 1. *For any $u \in V_p$, there is a stable sub-space decomposition $u_p = u_0 + \sum_{V \in \mathcal{V}} u_V$ such that*

$$\|u_0\|_A^2 + \sum \|u_V\|_A^2 \preceq \|u\|_A^2$$

For hexes: Pavarino [96], for triangles: Melenk+Eibner [04]
New result for tets: together with Melenk+Pechstein+Zaglmayr [DD16]

Step 1: Coarse grid contribution

Subtract a coarse grid quasi-interpolant:

$$u_1 = u - \Pi_0 u$$

by estimates of the Clément operator:

$$\|\nabla u_1\|^2 + \|h^{-1} u_1\|^2 \preceq \|u\|_A^2$$

Step 2: Vertex contribution by spider averaging

level sets of vertex functions

$$\gamma_V(s) := \{y \in \omega_V : \varphi_V(y) = s\}$$

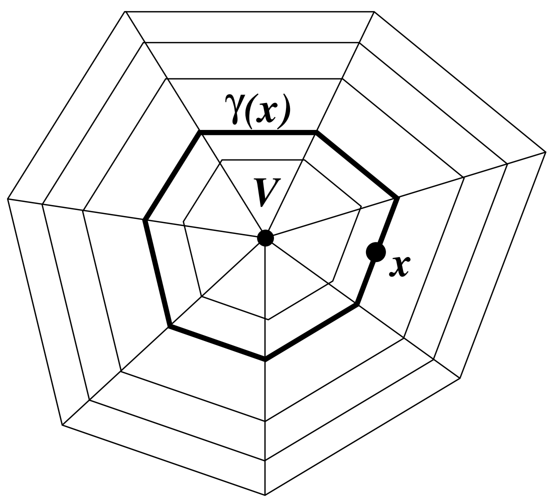

multi-dimensional vertex space

$$S_V := \{w \in V_p : w|_{\gamma_V(s)} = \text{const}\} = \mathrm{span}\{1, \varphi_V, ..., \varphi_V^p\}$$

Spider vertex averaging operator

$$\big(\Pi^V v\big)(x) := \frac{1}{|\gamma_V(x)|} \int_{\gamma_V(x)} v(y)\, dy,$$

It satisfies $\Pi^V V_p = S_V$, preservers vertex values $(\Pi^V u)(V) = u(V)$, and is continuous in the sense

$$\|\nabla\, \Pi^V u\|_{L_2(\omega_V)} + \|r_V^{-1}\{u - \Pi^V u\}\|_{L_2(\omega_V)} \preceq \|\nabla u\|_{L_2(\omega_V)}$$

Spider averaging with boundary values

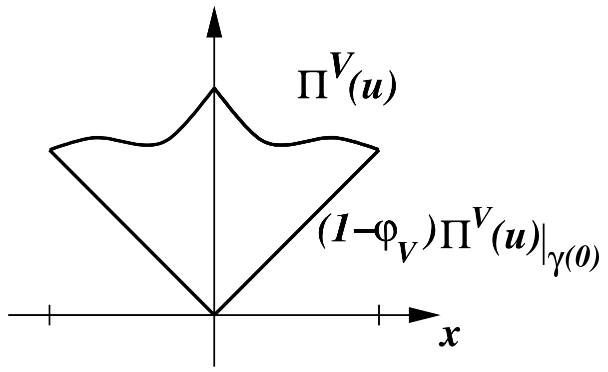

$$S_{V,0} := \{w \in S_V : w = 0 \text{ on } \gamma(0)\} = \mathrm{span}\{\varphi_V, ..., \varphi_V^p\}$$

Dirichlet spider vertex operator

$$\big(\Pi_0^V v\big)(x) := \big(\Pi^V v\big)(x) - (\Pi^V v)|_{\gamma_V(0)}(1 - \varphi_V(x)).$$

It satisfies $\Pi_0^V V_p = S_{V,0}$, preservers vertex values $(\Pi_0^V u)(V) = u(V)$, and is continuous in the sense

$$\|\nabla\, \Pi_0^V u\|_{L_2(\omega_{V,0})} + \|r_{\mathcal{V}}^{-1}\{u - \Pi_0^V u\}\|_{L_2(\omega_V)} \preceq \|\nabla u\|_{L_2(\omega_V)} + \|h^{-1} u\|_{L_2(\omega_V)}$$

with $r_{\mathcal{V}}(x) := \min\{|x - V| : V \in \mathcal{V}\}$

The global vertex interpolator

Global vertex interpolator:

$$\Pi_{\mathcal{V}} := \sum_{v\in\mathcal{V},\, v\notin\Gamma_D} \Pi_0^V$$

Lemma: The decomposition

$$u_1 = \underbrace{(u_1 - \Pi_{\mathcal{V}} u_1)}_{=:u_2} + \sum_V \Pi_0^V u_1$$

is stable in the sense of

$$\|\nabla u_2\|^2 + \|r_{\mathcal{V}}^{-1} u_2\|^2 + \sum_V \|\Pi_0^V u_1\|_A^2 \preceq \|\nabla u_1\|^2 + \|h^{-1} u_1\|^2.$$

We have subtracted multi-dimensional vertex functions in $S_{V,0} \subset V_V$. The rest u_2 satisfies well-defined 0-values in the vertices.

Step 3: Decompositon of edge-contributions

Lemma: There holds the trace estimate

$$\sum_{E\in\mathcal{E}} \|u_2\|^2_{H^{1/2}_{00}(E)} \preceq \|\nabla u_2\|^2 + \|r_{\mathcal{V}}^{-1} u_2\|^2$$

The Munoz-Sola extension $R_{E\to T}$ is a bounded extension operator from $H^{1/2}_{00}(E)$ to $H^1(T)$ preserving polynomials, and 0-boundary values on the other 2 edges:

Define the edge interpolation operator $\Pi_E : V_{u_v=0} \to V_E$ as

$$\Pi_E u = R_{E\to T}\, \mathrm{tr}_E\, u,$$

and decompose

$$u_2 = \underbrace{u_2 - \sum_{E\in\mathcal{E}} u_2}_{=:u_3} + \sum_{E\in\mathcal{E}} u_2$$

Then, $u_3 = 0$ on $\cup E$, and

$$\|u_3\|^2_{H^1} + \sum_{E\in\mathcal{E}} \|\Pi_E u_2\|^2_A \preceq \|\nabla u_2\|^2 + \|r_{\mathcal{V}}^{-1} u_2\| \preceq \|u\|^2_A.$$

The Spidervertex-Edge-Inner space splitting

With $u \in V_P$, $u_1 = \Pi_0 u$, $u_2 = u_1 - \sum_{V \in \mathcal{V}} \Pi_0^V u_1$, $u_3 = u_2 - \sum_{E \in \mathcal{E}} \Pi_0^E u_2$,

the decomposition

$$u = u_0 + \sum_{V \in \mathcal{V}} \Pi_0^V u_1 + \sum_{E \in \mathcal{E}} \Pi_0^E u_2 + \sum_{T \in \mathcal{T}} u|_T$$

is stable in H^1.

Each of the vertex, edge, and element contribution is contained in one of the overlapping vertex patches, thus the overlapping Schwarz method is robust in p.

Low energy vertex basis functions

[Ion Bica 97], [Sherwin + Casarin 02] Implicit low energy basis functions
The optimal low energy vertex interpolant into $S_{V,0}$ is defined by

$$\min_{\substack{w \in S_{V,0} \\ w(V)=u(V) \quad w=0 \text{ on } \gamma(0)}} \|w\|_{H^1},$$

By setting $w(x) = v(\varphi_V(x))$, this is a 1D problem with weighted norms

$$\min_{v \in P^p : v(1)=1, v(0)=0} \int_0^1 (1-s)\big(v'(s)\big)^2 \, ds.$$

In terms of Jacobi polynomials $P_i^{0,-1}$, its solution is

$$v(x) = \Big(\sum_{i=1}^{p} \frac{1}{i}\Big)^{-1} \sum_{i=1}^{p} \frac{1}{i} P_i^{0,-1}(2x-1)$$

Then, the explicit 2D low energy vertex function is

$$w(x) = v(\varphi_V(x)).$$

Computational results in 2D

Solve $(\nabla u, \nabla v) + (u, v)_{\partial\Omega} = (1, v)$ on $(0, 1)^2$
eliminate internal bubbles

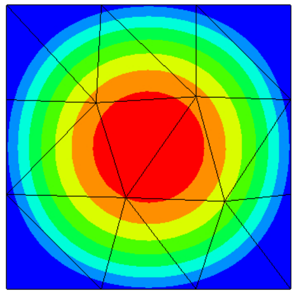

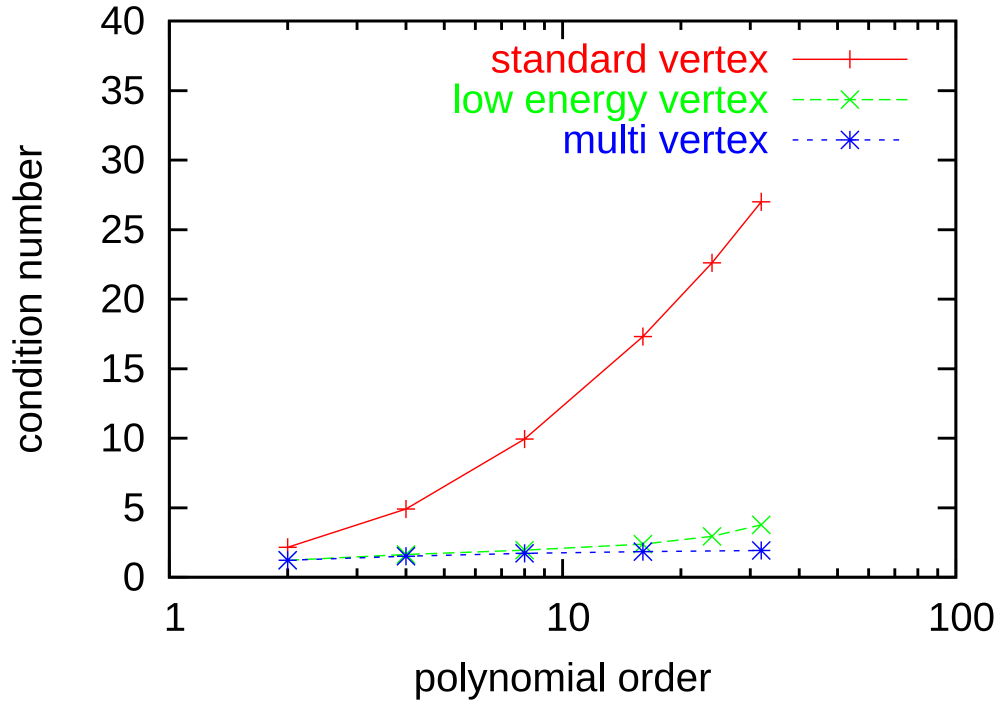

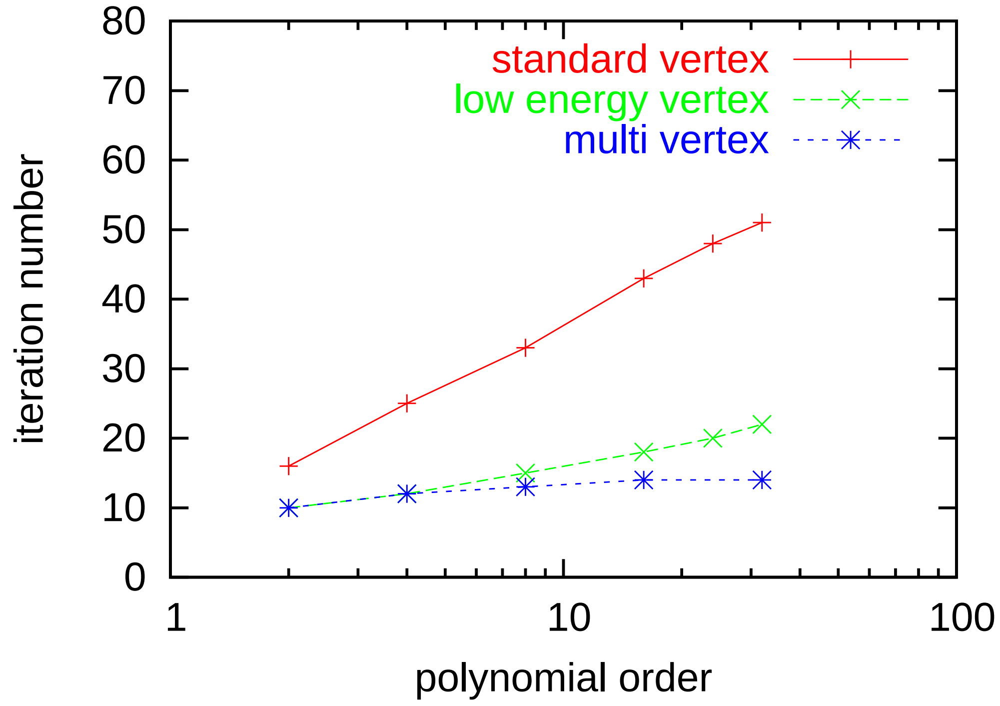

Additive Schwarz on tetrahedra

Very similar as in 2D:

- Spider vertex spaces on level set surfaces:

$$\begin{aligned} \Gamma_V(x) &= \{y : \varphi_V(y) = \varphi_V(x)\} \\ S_{V,0} &= \{w \in V_{V,0} : w|_{\Gamma_V(x)} = \mathsf{const}\} = \mathrm{span}\{\varphi_V, ..., \varphi_V^p\} \end{aligned}$$

- Spider edge spaces for edge $E = (e_1, e_2)$ on level set curves:

$$\begin{aligned} \gamma_E(x) &= \{y : \varphi_{e_i}(y) = \varphi_{e_i}(x),\ i = 1, 2\} \\ S_{E,0} &= \{w \in V_{E,0} : w|_{\gamma_E(x)} = \mathsf{const}\} = \mathrm{span}\{p(\varphi_{e_1}(x), \varphi_{e_2}(x)) : p(s,t) \in stP^{p-2}(s,t)\} \end{aligned}$$

Stable AS subspace decompositions

- Spider-vertex space (p-dim)
  Spider-edge spaces (p^2-dim)
  Face spaces with Munoz-Sola extension (p^2-dim)
  Element spaces (p^3-dim)

$$V_p = V_0 + \sum_V S_{V,0} + \sum_E S_{E,0} + \sum_F W_F + \sum_T V_T$$

- Spider-vertex space (p-dim)
  Overlapping spaces on edge-patches (p^3-dim)

$$V_p = V_0 + \sum_V S_{V,0} + \sum_E V_{E,0}$$

Computational results in 3D, Overlapping edge blocks

solve $(\nabla u, \nabla v) + (u, v)_{\partial\Omega} = (1, v)$ on $(0,1)^3$
Mesh of 44 elements, elimination of internal bubbles,

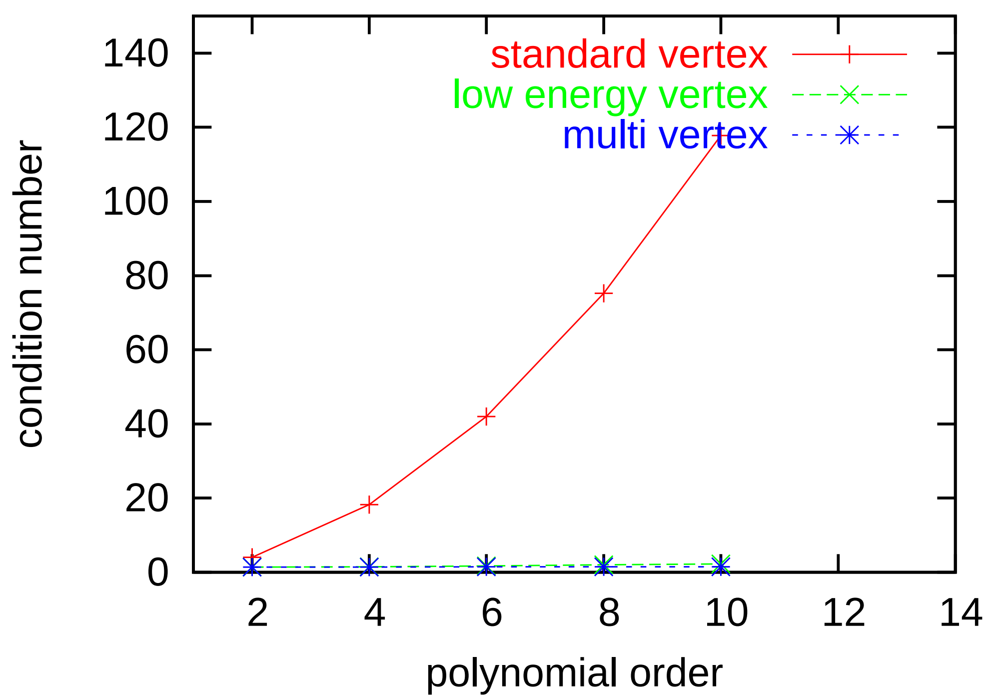

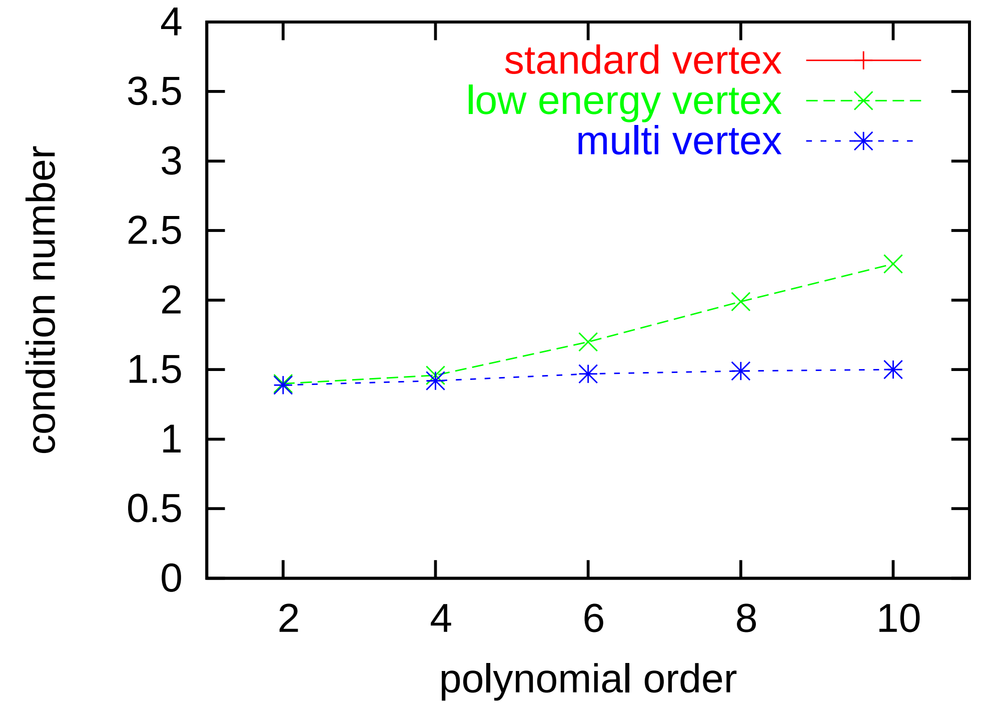

Polynomial preserving explicit extension from one edge

Step 1: Extension $H^{1/2}(E) \to H^1(T)$

$$u(x,y) := \frac{1}{2y} \int_{x-y}^{x+y} u_E(s)\, ds$$

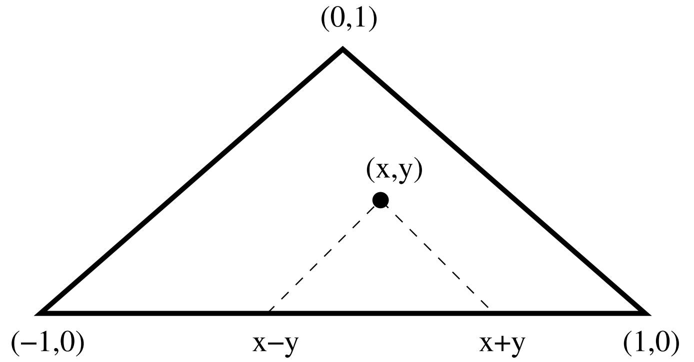

[Babuška+Craig+Mandel+Pitkäranta, 91]

Step 2: Preserving boundary conditions by blending

$H_{00}^{1/2}(E) \to H^1_{0,\partial T \setminus E}(T)$

upper right edge:

$$\hat{u}(x,y) = u(x,y) - \frac{2y}{1-x+y} u\left(\frac{1+x-y}{2}, \frac{1-x+y}{2}\right),$$

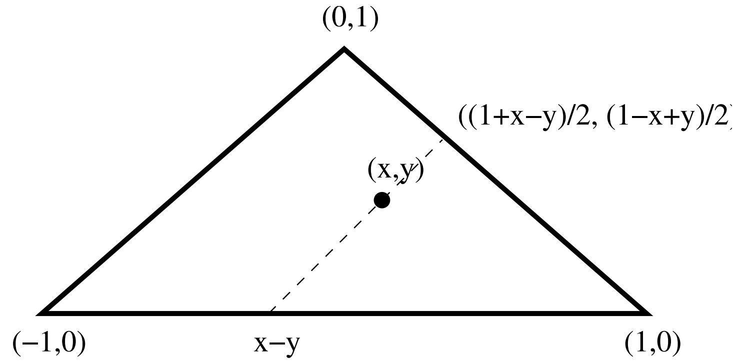

and similar for upper left edge.
Alternative to [Munoz-Sola, 97]

Explicit low energy edge-based shape functions

Define edge-based basis function as

$$\varphi_i(x,y) := [E\,P_i^{(2,2)}](x,y),$$

where $x = \lambda_1 - \lambda_2$, and $y = \lambda_1 + \lambda_2$.

P. Paule, A. Riese, C. Schneider, colleagues from the Linz-SFB "Numerical and Symbolic Scientific Computing": work on special function algorithms.

They could compute a 5-term reccurence for the evaluation of these basis-functions:

$$\mathbf{u_l}(x,y) = a_l \mathbf{u_{l-4}} + b_l x \mathbf{u_{l-3}} + (c_l + d_l(x^2 - y^2))\mathbf{u_{l-2}} + e_l x \mathbf{u_{l-1}}$$

The coefficients a_l, b_l, c_l, d_l, e_l are rational in l and are computed once and for all.

Non-overlapping AS: Computational results in 3D

- explicit low energy vertex functions
- elimination of inner variables
- edge functions: standard vs explicit low energy

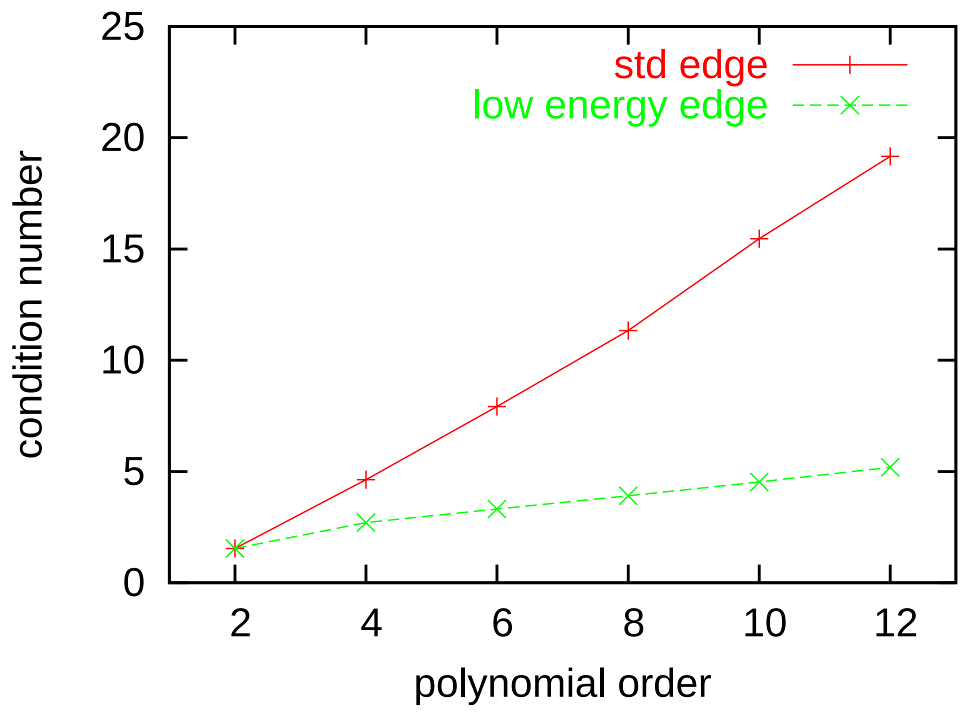

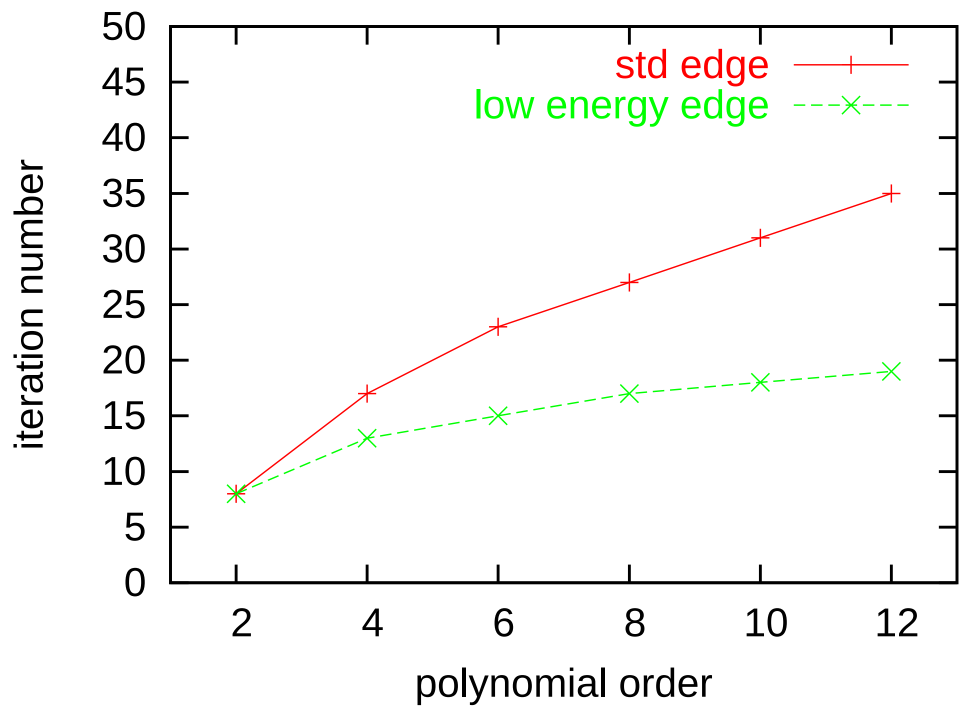

The p-version and hp-version FEM on a simple example

Example: Electric field in a plate capacitor

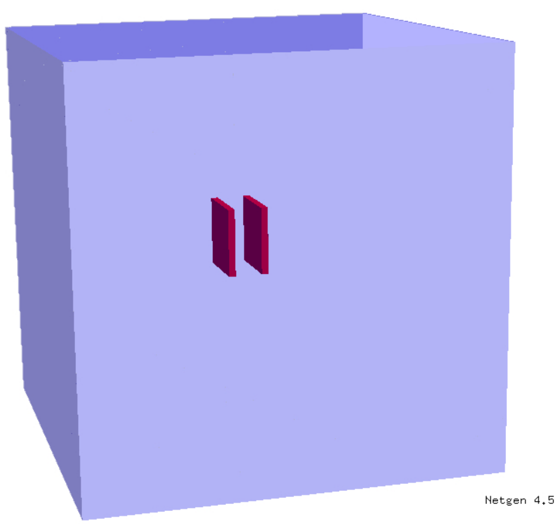

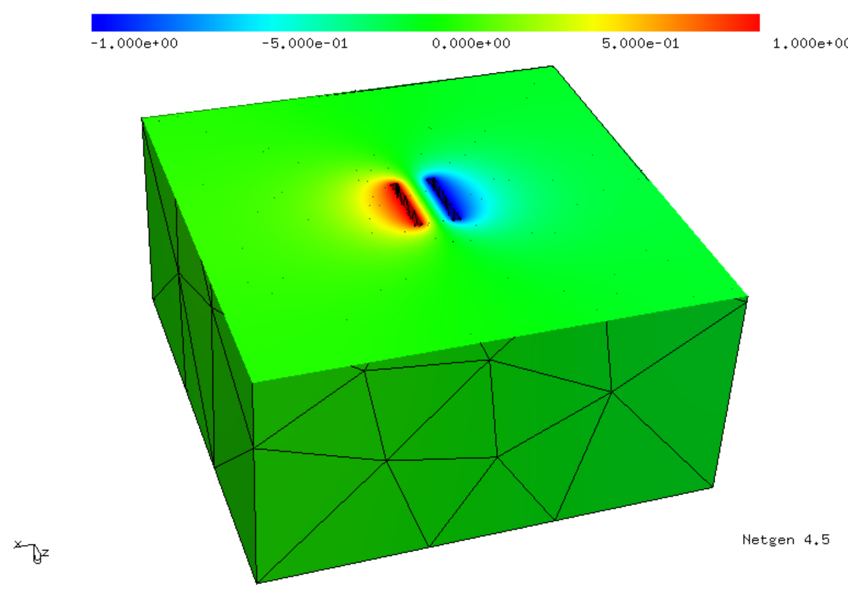

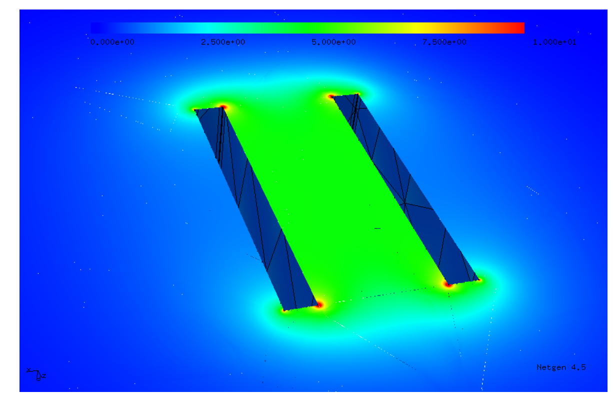

Geometry

Electrostatic Potential

Absolut value of the E-field

Higher order FEM in 2D

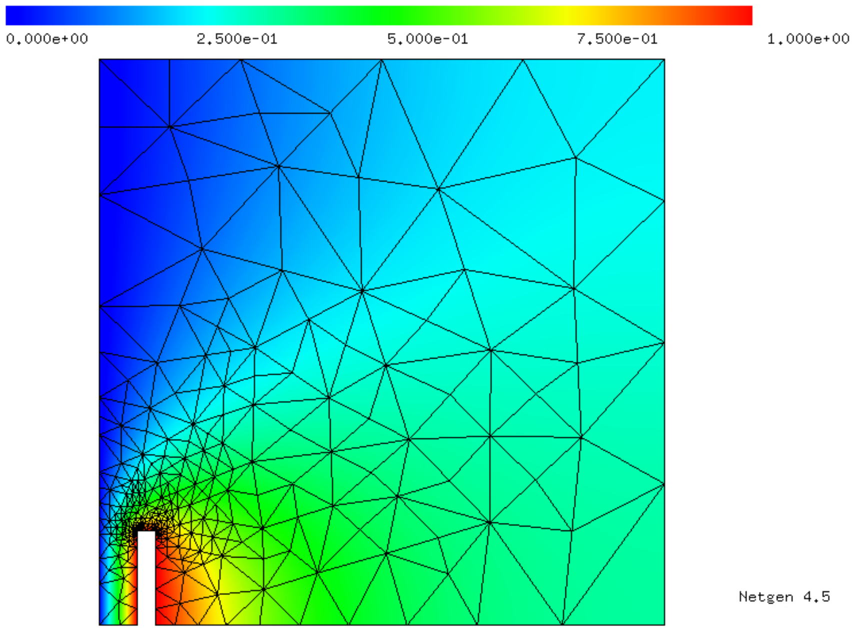

Adaptive mesh and potential
Based on ZZ error estimator

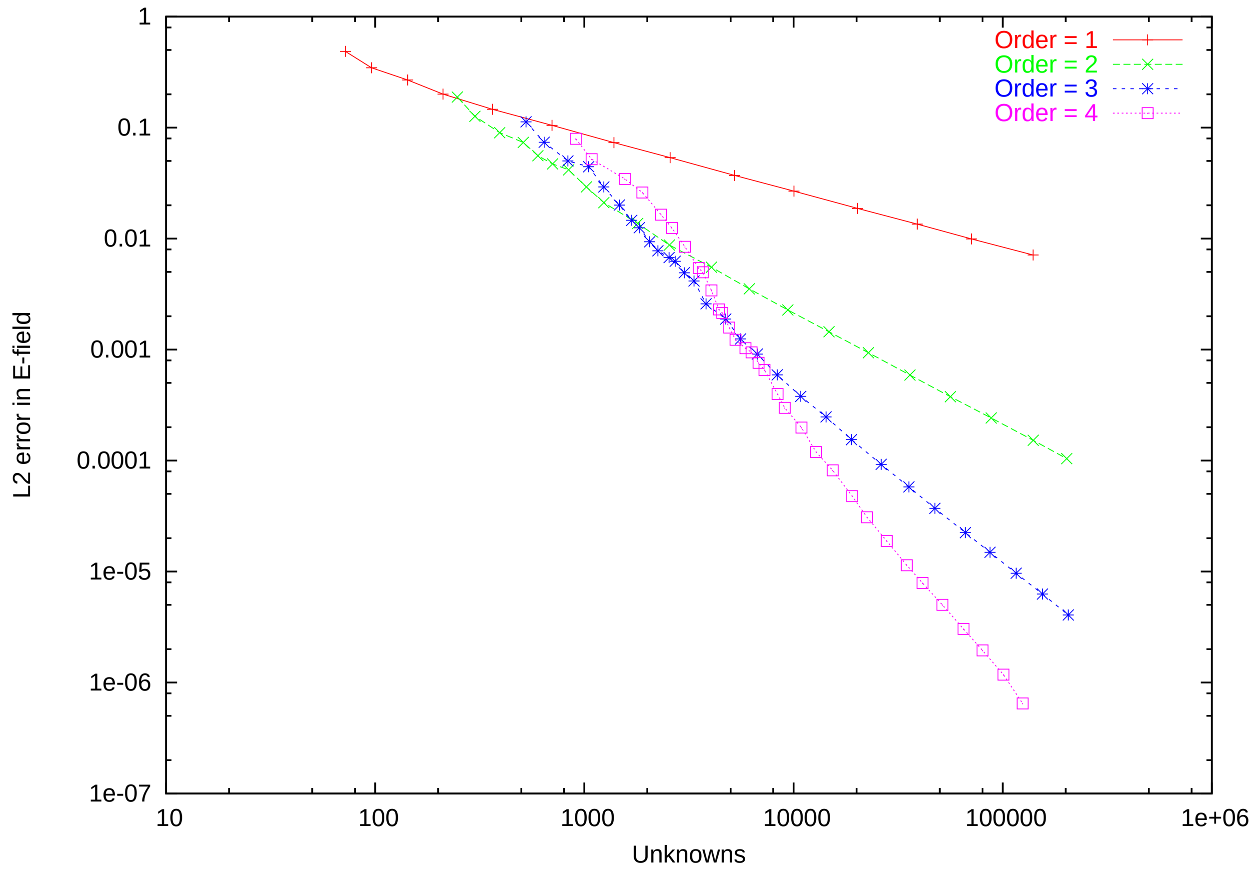

Adaptive hp-FEM in 2D

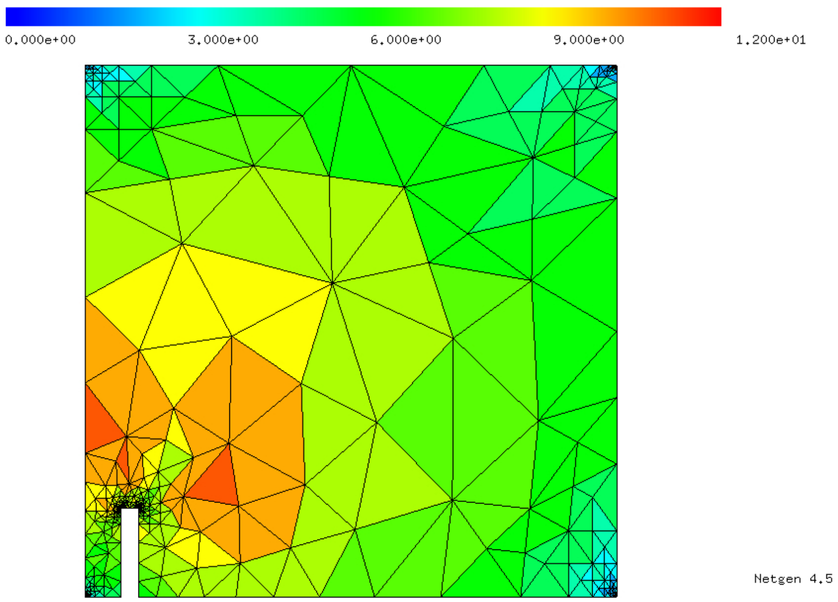

Variable polynomial order based on ZZ error estimator

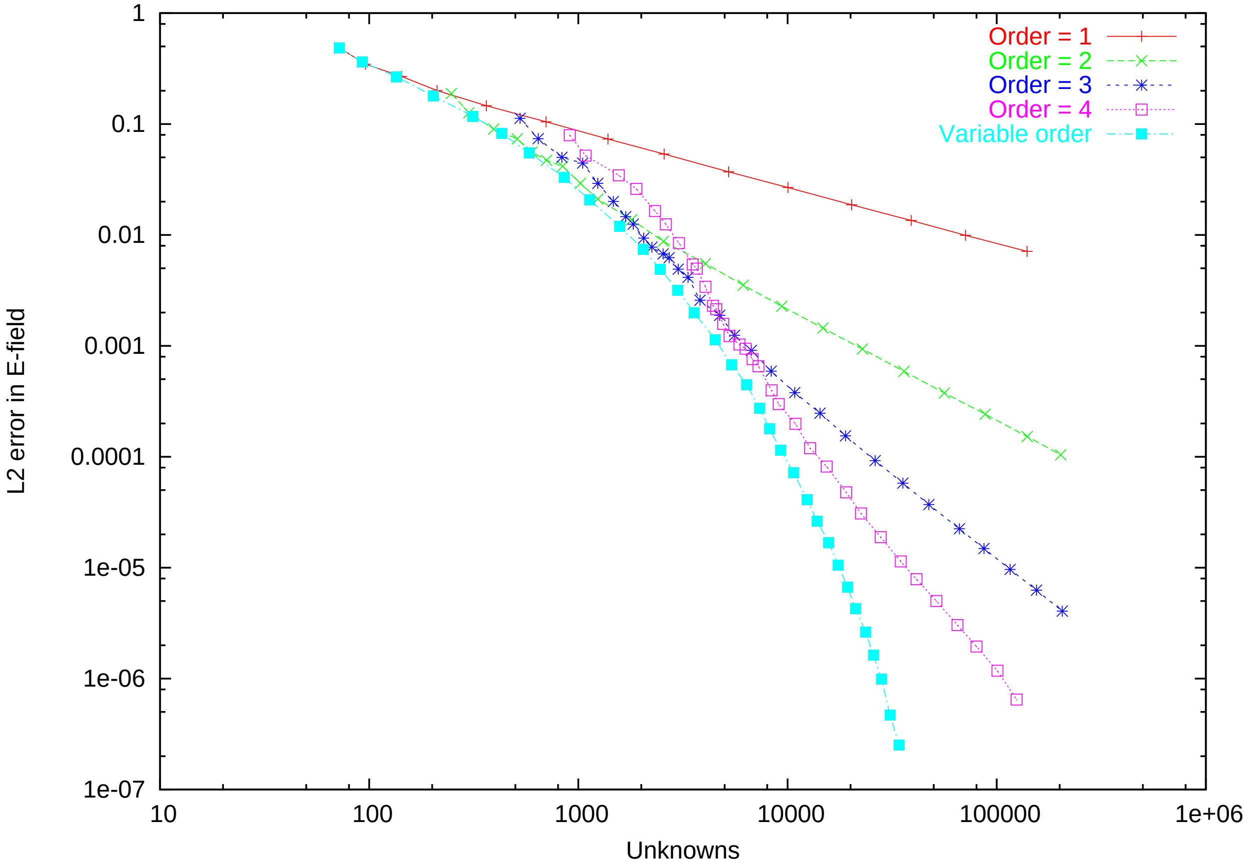

Adaptive high order FEM in 3D

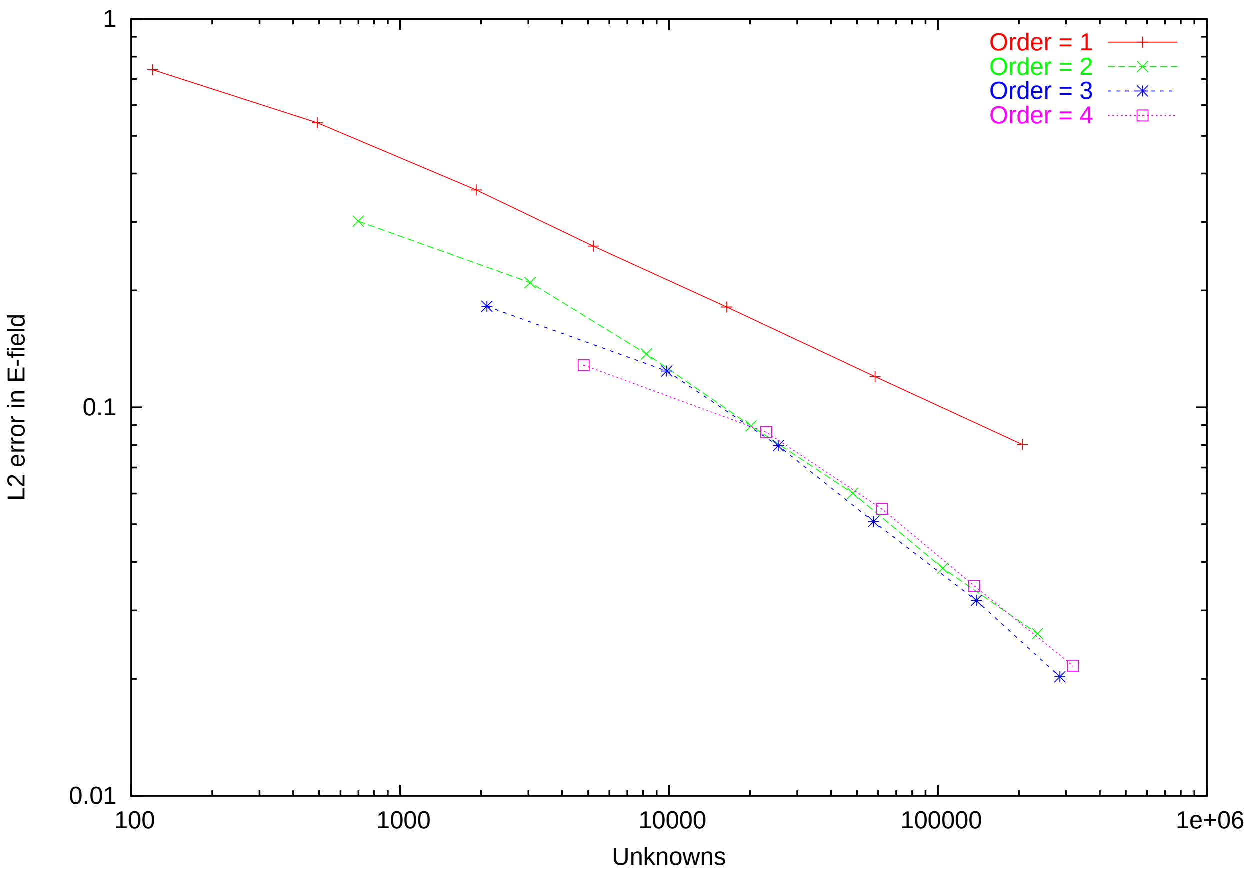

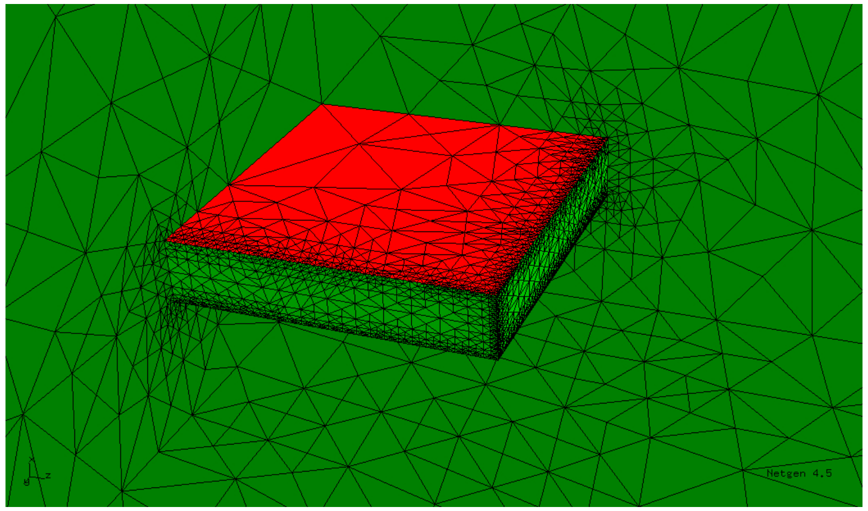

mesh refinement based on ZZ error estimator

hp-FEM in 3D

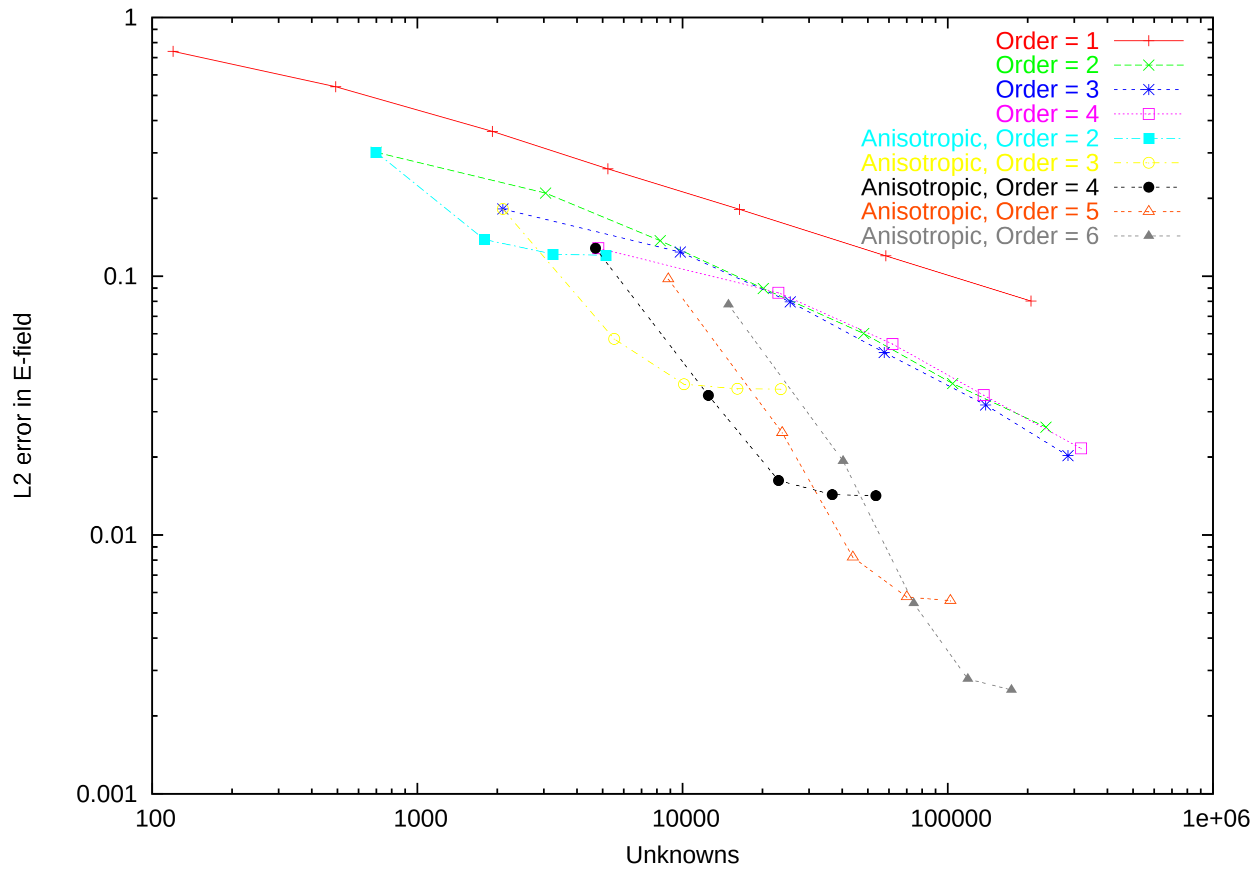

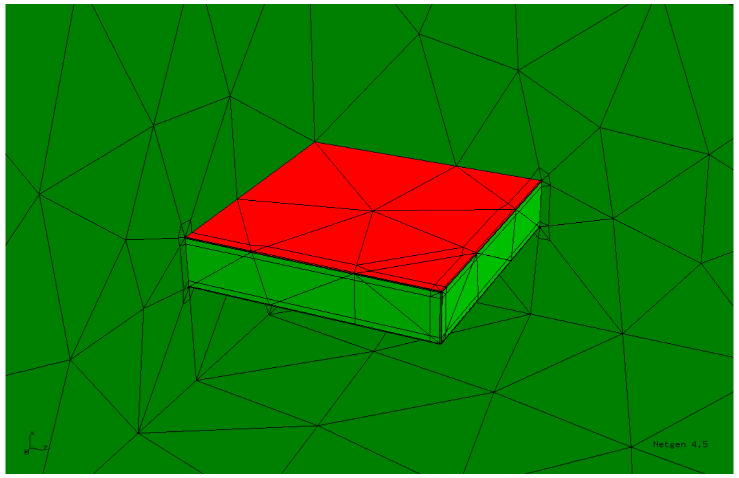

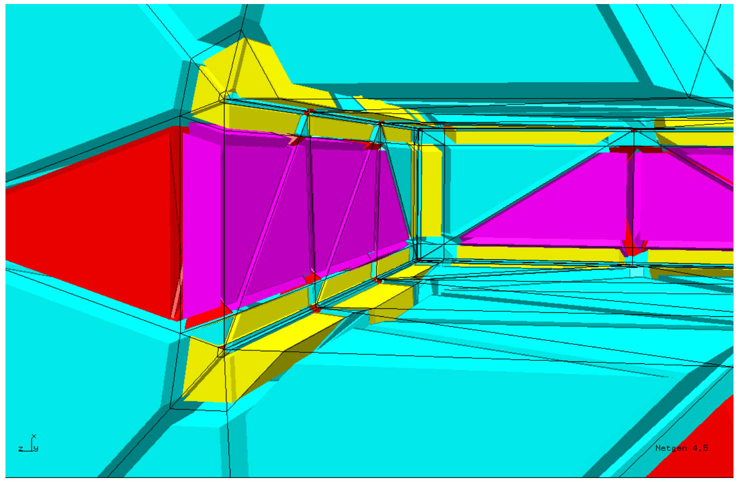

a priori anisotropic mesh refinement

[Babuška, Schwab, Guo, Dauge, Costabel, Apel, ...]

Template based geometric mesh refinement

- Generate initial tetrahedral mesh, and mark a priori singular corners and edges
- Perform k steps of geometric mesh refinement

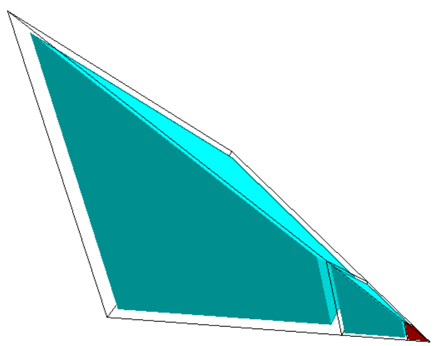

1 singular vertex

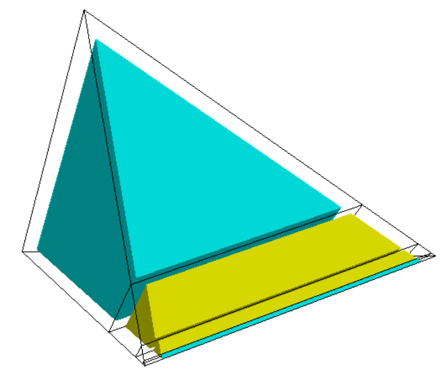

1 singular edge

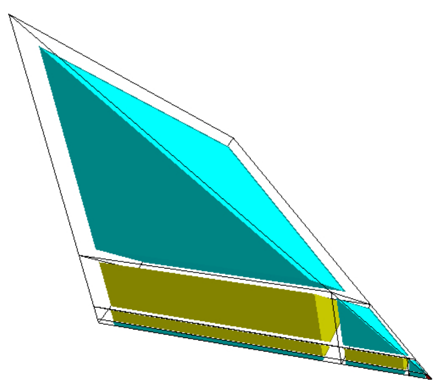

1 sing v + 1 sing e

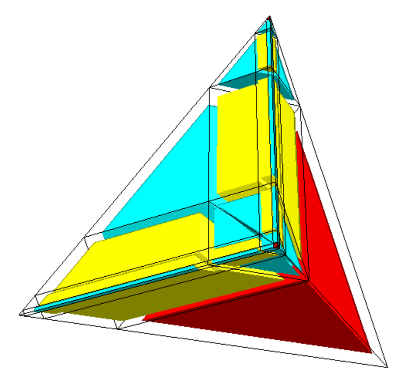

2 sing v + 2 sing e

AS decomposition for anisotropic edge refinement

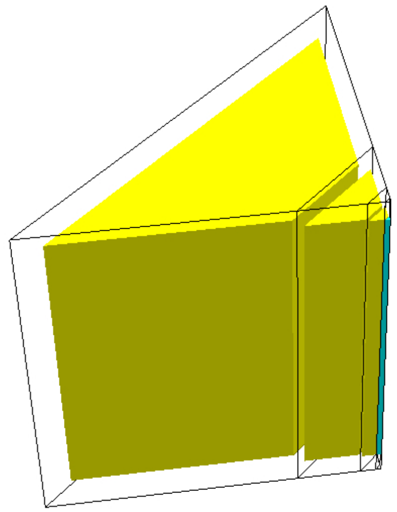

Is plane smoothing necessary ?

Finite element stiffness matrix:

$$A = A_{xy} \otimes M_z + M_{xy} \otimes A_z$$

Local ASM-preconditioners for 2D problems:

$$C_{xy}^A = \mathrm{blockdiag}\, A_{xy} \qquad C_{xy}^M = \mathrm{blockdiag}\, M_{xy}$$

3D ASM-preconditioner:

$$C = C_{xy}^A \otimes M_z + C_{xy}^M \otimes A_z$$

2D problem: coarsegrid only 1 triangle, standard vertex shape functions, static condensation:

$$\kappa = O(l^2 + p^\alpha) \qquad (\alpha = 2?)$$

Computations on prismatic domain with 1 singular edge

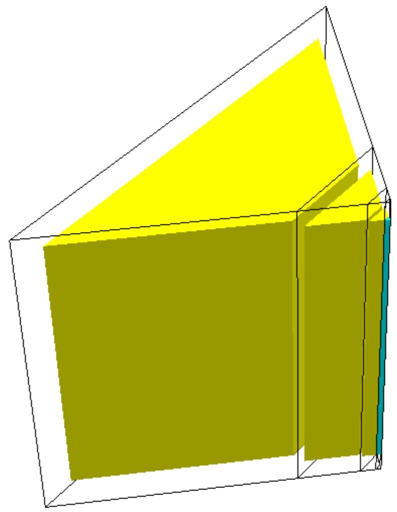

h-refinement level $L = 0, \ldots 5$
element aspect ratio $= 8^L$. $\quad (8^5 = 32768)$

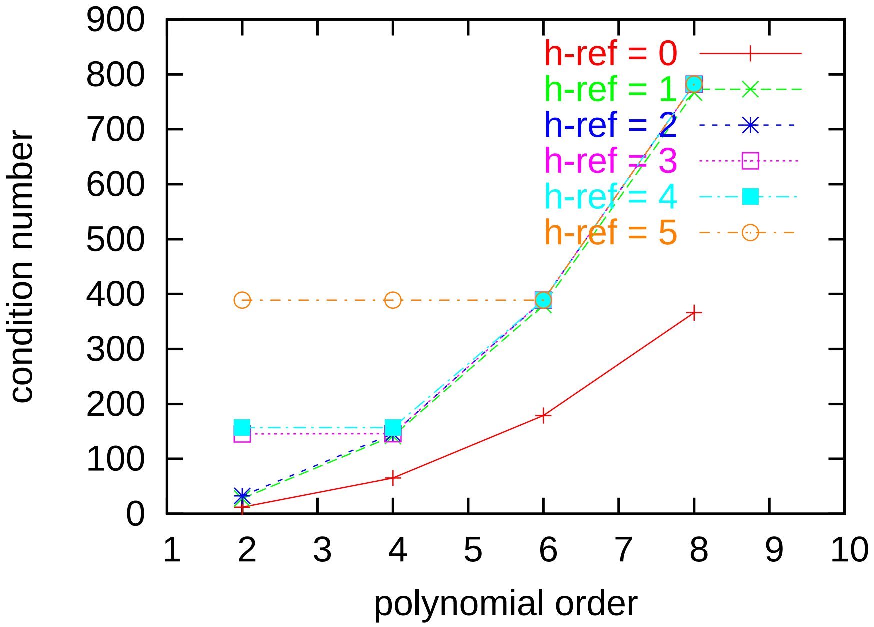

Poisson problem on a crank shaft

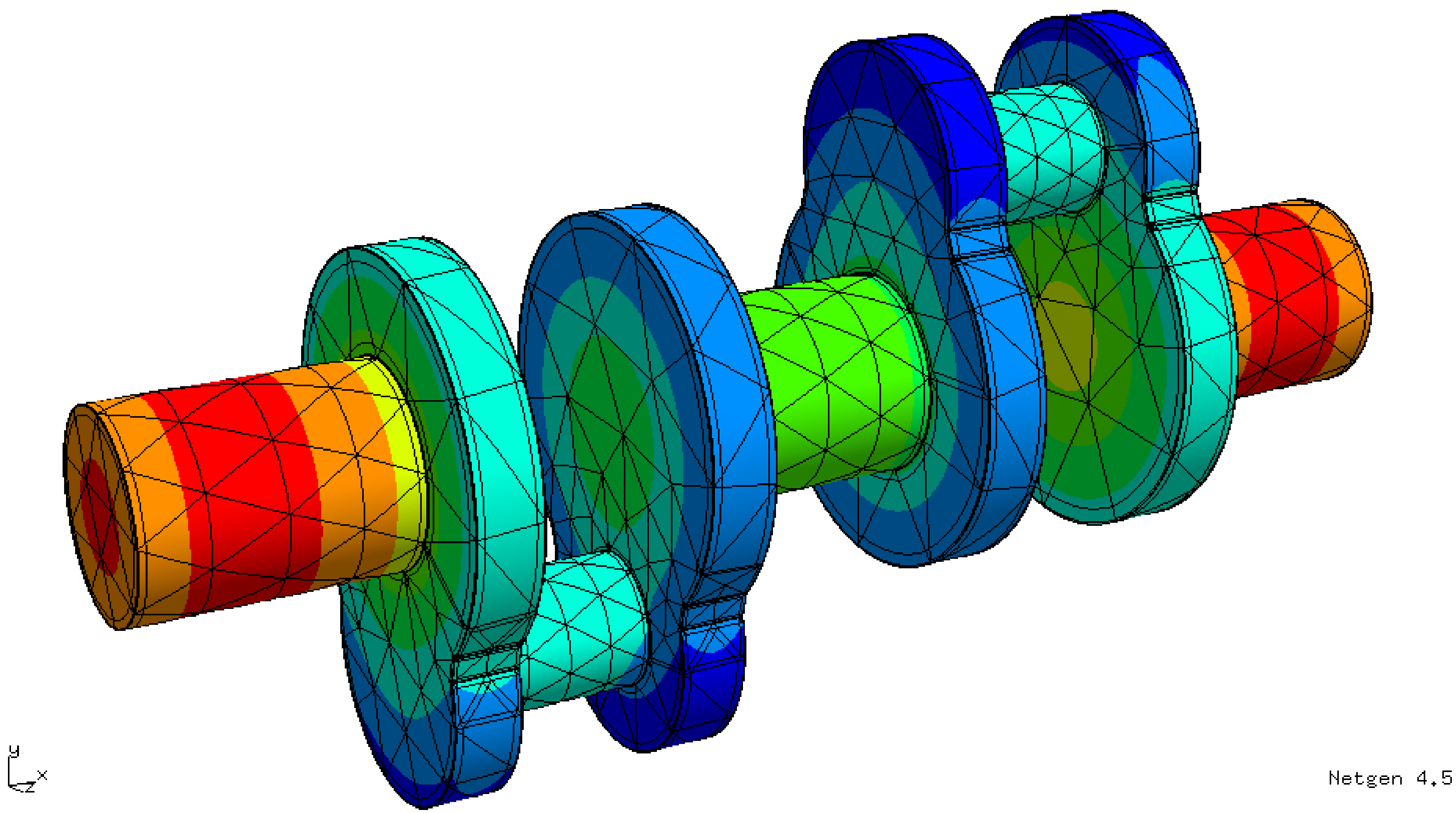

2 levels h-ref, $p = 4$, $N = 209664$, 32 iterations, solver: 52 sec, total 203 sec (1.7 GHz notebook)

Maxwell equations

Time harmonic setting:

$$\begin{aligned} \text{curl } H &= j_i + \sigma E + i\omega\varepsilon E, \\ \text{curl } E &= -i\omega\mu H. \end{aligned}$$

By introducing the magnetic vector potential $A = \frac{-1}{i\omega}E$, there follows

$$H = \frac{-1}{i\omega\mu}\,\text{curl } E = \mu^{-1}\ \text{curl } A$$

Strong vector potential formulation:

$$\text{curl } \mu^{-1}\,\text{curl } A + i\omega\sigma A - \omega^2\varepsilon A = j_i$$

with boundary conditions:

$$A \times n = 0, \qquad \text{or} \qquad (\mu^{-1}\,\text{curl } A) \times n = j_s, \qquad \text{or} \qquad (\mu^{-1}\,\text{curl}\, A) \times n = \kappa(A \times n)$$

Variational problems in $H(\mathrm{curl})$

Function space

$$H(\mathrm{curl}) := \{u \in [L_2]^3 : \mathrm{curl}\ u \in [L_2]^3\}$$

Magnetostatic/Eddy-current problem in weak form:

Find vector potential $A \in H(\mathrm{curl})$ such that

$$\int_\Omega \mu^{-1}\,\mathrm{curl}\ A \cdot \mathrm{curl}\ v\,dx + \int_\Omega i\omega\sigma\,A \cdot v\,dx = \int_\Omega j \cdot v\,dx \qquad \forall\, v \in H(\mathrm{curl}),$$

Gauging by regularization in insulators

Maxwell eigenvalue problem:

Find eigenfrequencies $\omega \in \mathbb{R}_+$ and $E \in H(\mathrm{curl})$ such that

$$\int_\Omega \mu^{-1}\ \mathrm{curl}\ E \cdot \mathrm{curl}\ v\,dx = \omega^2 \int_\Omega \varepsilon\,E \cdot v\,dx \qquad \forall\, v \in H(\mathrm{curl})$$

The de Rham Complex

$$
\begin{array}{ccccccc}
H^1 & \xrightarrow{\nabla} & H(\mathrm{curl}) & \xrightarrow{\mathrm{curl}} & H(\mathrm{div}) & \xrightarrow{\mathrm{div}} & L^2 \\
\bigcup & & \bigcup & & \bigcup & & \bigcup \\
W_h & \xrightarrow{\nabla} & V_h & \xrightarrow{\mathrm{curl}} & Q_h & \xrightarrow{\mathrm{div}} & S_h
\end{array}
$$

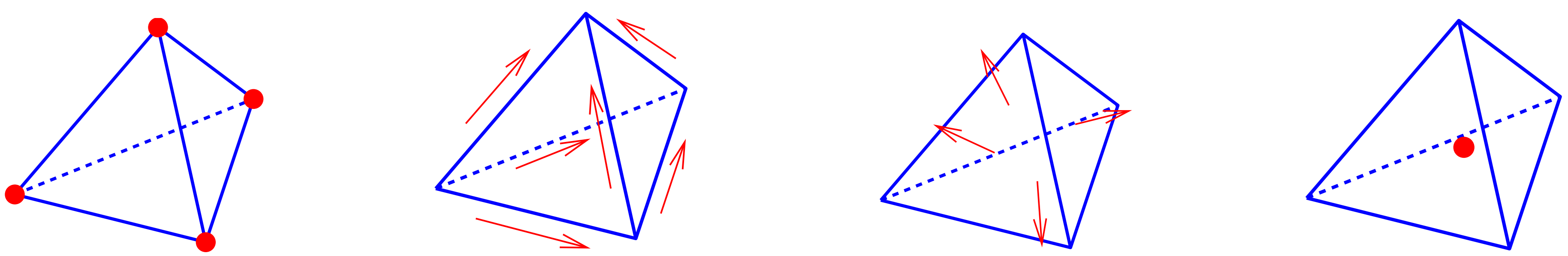

satisfies the **complete sequence property**

$$
\begin{aligned}
\mathrm{range}(\nabla) &= \ker(\mathrm{curl}) \\
\mathrm{range}(\mathrm{curl}) &= \ker(\mathrm{div})
\end{aligned}
$$

on the continuous and the discrete level.

Important for stability, error estimates, preconditioning, ...

Magnetic field induced by a coil (magnetostatics)

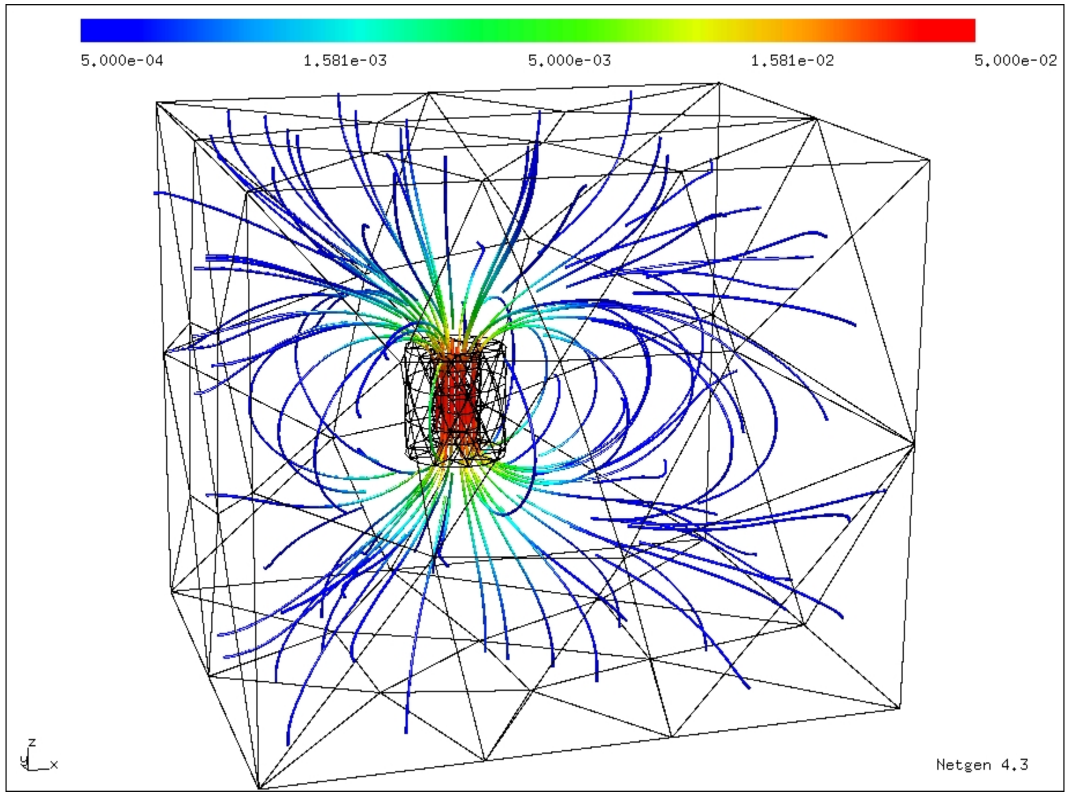

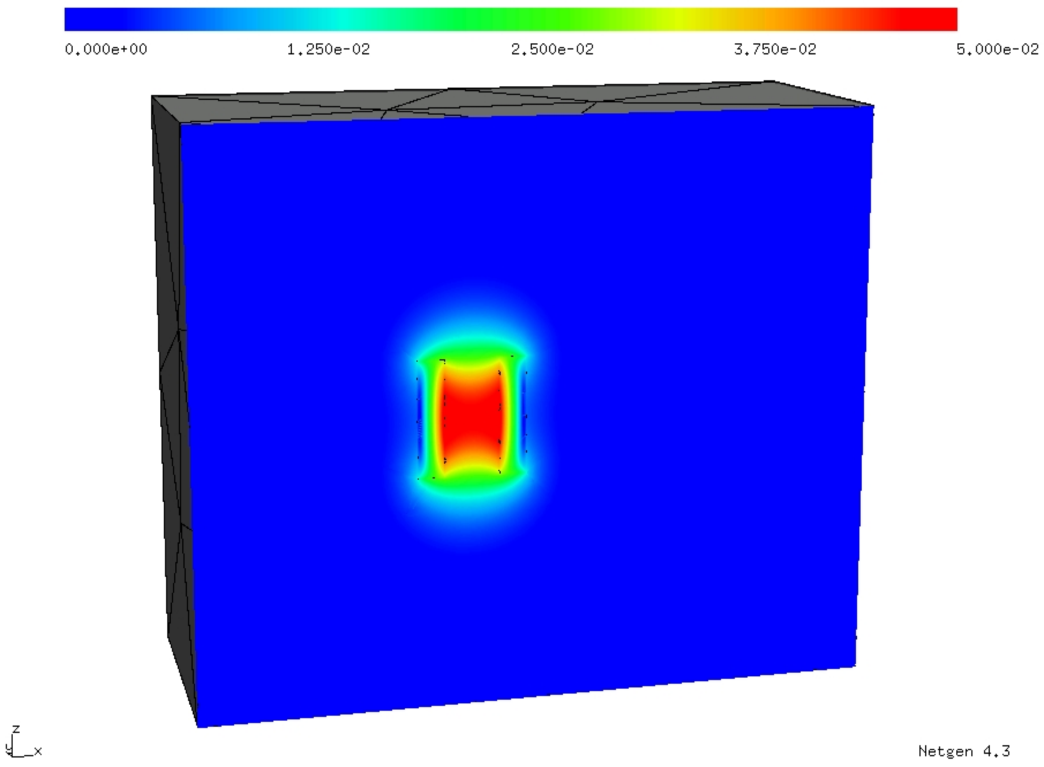

Netgen/NGSolve

2035 Nédélec-II tets, $p = 6$, 186 470 unknowns, 59 PCG-its, 87 sec solver time

On the construction of high order finite elements

- [Dubiner, Karniadakis+Sherwin] H^1-conforming shape functions in tensor product structure
  $\rightarrow$ allows fast summation techniques

- [Webb] $H(\mathrm{curl})$ hierarchic shape functions with local complete sequence property
  convenient to implement up to order 4

- [Demkowicz et al] Based on global complete sequence property construction of Nédélec elements of variable order (with constraints on order distribution) for hexahedra

- [Ainsworth+Coyle] Systematic construction of $H(\mathrm{curl})$-conforming elements of arbitrarily high order for tetrahedra

- [Schöberl+Zaglmayr] Based on **local complete sequence property** and by using **tensor-product structure** we achieve a **systematic strategy** for the construction of $H(\mathrm{curl})$-conforming hierarchic shape functions of **arbitrary** and **variable order for common element geometries** (segments, quadrilaterals, triangles, hexahedra, tetrahedra, prisms).
  [JS + Zaglmayr, Compel, 2005]

The deRham Complex tells us that $\nabla H^1 \subset H(\mathrm{curl})$, as well for discrete spaces $\nabla W^{p+1} \subset V^p$.

Vertex basis function

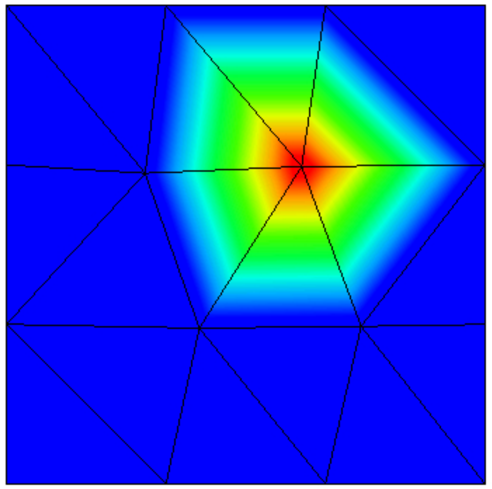

Edge basis function p=3

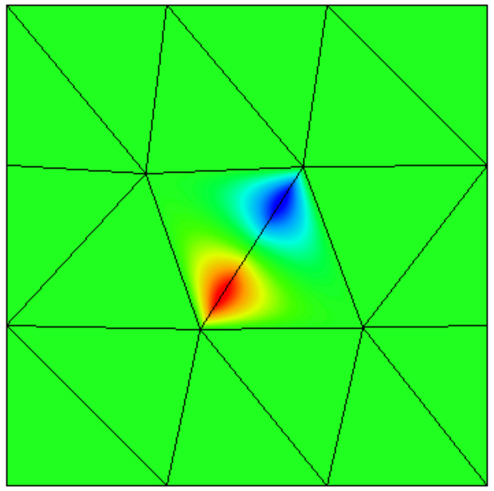

Inner basis function p=3

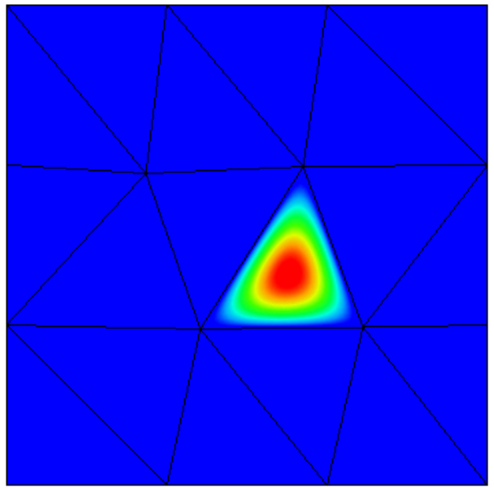

The deRham Complex tells us that $\nabla H^1 \subset H(\mathrm{curl})$, as well for discrete spaces $\nabla W^{p+1} \subset V^p$.

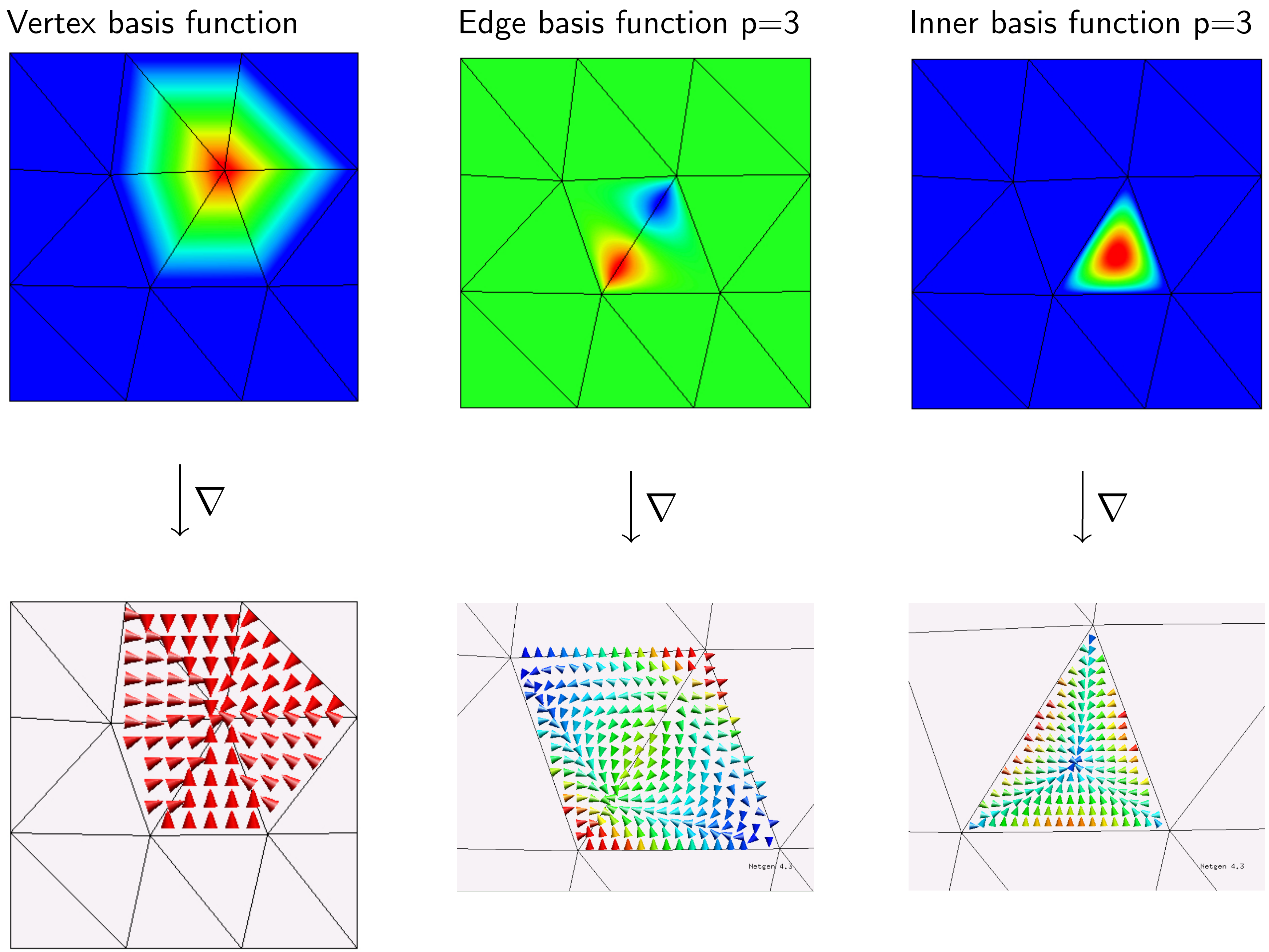

$\nabla W_{V_i} \subset V_{\mathcal{N}_0}$ $\nabla W^{p+1}_{E_k} = V^p_{E_k}$ $\nabla W^{p+1}_{F_k} \subset V^p_{F_k}$

Localized complete sequence property

We have constructed **V**ertex-**E**dge-**F**ace-**I**nner shape functions satisfying

$$
\begin{array}{lllllll}
W^V_{h,\,p+1=1} & \xrightarrow{\nabla} V_h^{\mathcal{N}_0} & \xrightarrow{\text{curl}} & Q_h^{\mathcal{RT}_0} & \xrightarrow{\text{div}} & S_{h,\,0} \\
W^E_{p_E+1} & \xrightarrow{\nabla} V^E_{p_E} & & & & \\
W^F_{p_F+1} & \xrightarrow{\nabla} V^F_{p_F} & \xrightarrow{\text{curl}} & Q^F_{p_F-1} & & \\
W^I_{p_I+1} & \xrightarrow{\nabla} V^I_{p_I} & \xrightarrow{\text{curl}} & Q^I_{p_I-1} & \xrightarrow{\text{div}} & S^I_{p_I-2}.
\end{array}
$$

Advantages are

- allows arbitrary and variable polynomial order on each edge, face and cell
- Additive Schwarz Preconditioning with cheap $\mathcal{N}_0 - E - F - I$ blocks gets efficient
- Reduced-basis gauging by skipping higher-order gradient bases functions
- discrete differential operators B_∇, B_{curl}, B_{div} are trivial

Robust preconditioners for $H(\mathrm{curl})$

The finite element discretization of

$$A(u,v) = \int \operatorname{curl} u \cdot \operatorname{curl} v + \varepsilon\, u \cdot v \, dx$$

leads to the matrix $A = K + \varepsilon M$, where the kernel of K corresponds to the gradients of the H^1-finite elements:

$$V_0 = \nabla W_h$$

An ε-robust additive Schwarz preconditioner must fulfill

$$V_h = \sum V_i \qquad \text{and} \qquad V_0 = \sum V_i \cap V_0$$

Let $W = \sum W_i$ the decomposition w.r.t. the nodal basis functions. Then $V_0 = \sum \nabla W_i$. The preconditioner is robust if one chooses V_i such that

$$\forall W_i \, \exists V_j \; : \; \nabla W_i \subset V_j$$

Two-level/Multigrid analysis for $H(\mathrm{curl})$

- Toselli: Overlapping DD methods on convex domains, FETI - DP
- Arnold-Falk-Winther: Multigrid for convex domain, robust in ε
- Hiptmair: Multilevel techniques, Lipschitz domains, non-robust in ε
- Pasciak + Zhao: Overlapping DD for Lipschitz domains, robust in ε

Partition of unity for $H(\mathrm{curl})$

Pasciak + Zhao: Helmholtz-like decomposition:

$$\underbrace{u}_{\in H(\mathrm{curl})} = \nabla \underbrace{\varphi}_{\in H^1} + \underbrace{z}_{\in [H^1]^3}$$

with global estimate:

$$\|\nabla \varphi\|_\Omega \leq c(\Omega) \|u\|_\Omega \qquad \|\nabla z\|_\Omega \leq c(\Omega) \|\operatorname{curl} u\|_\Omega$$

With Clément-type quasi-interpolation operator [JS, Report 01] to the coarse grid, and new estimates [JS, Report 05]

$$u - \Pi_H u = \nabla \underbrace{\varphi}_{\in H^1} + \underbrace{z}_{\in [H^1]^3}$$

with patch-wise local stability:

$$\|h^{-1} \varphi\|_{\omega_V} + \|\nabla \varphi\|_{\omega_V} \leq c(\omega_V) \|u\|_{\tilde{\omega}_V} \qquad \|h^{-1} z\|_{\omega_V} + \|\nabla z\|_{\omega_V} \leq c(\omega_V) \|\operatorname{curl} u\|_{\tilde{\omega}_V}$$

Reduced Basis Gauging for Magnetostatic problem

- regularization term for lowest-order subspace
- skipping higher-order gradient basis functions

Reduced-base vs. full-space regularization in simulation of coil-problem:

In reduced system about a third less shape functions $\rightarrow \approx 55\%$ faster integration

p	dofs	reduced/full	$\kappa(C^{-1}A)$	iterations	solver time
2	19719	full	7.9	20	1.9 s
2	10686	reduced	7.9	21	0.7 s
3	50884	full	24.2	32	9.8 s
3	29130	reduced	18.2	31	2.9 s
4	104520	full	71.4	48	40.5 s
4	61862	reduced	32.3	40	10.7 s
5	186731	full	179.9	69	137.9 s
5	112952	reduced	55.5	49	31.9 s
6	303625	full	421.0	97	427.8 s
6	186470	reduced	84.0	59	87.4 s
7	286486	reduced	120.0	68	209.6 s

Note: the computed $B = \mathrm{curl}\ A$ are the same for both versions.

Eddy-current Simulation of a bus bar

Time harmonic low fequency Maxwell equations

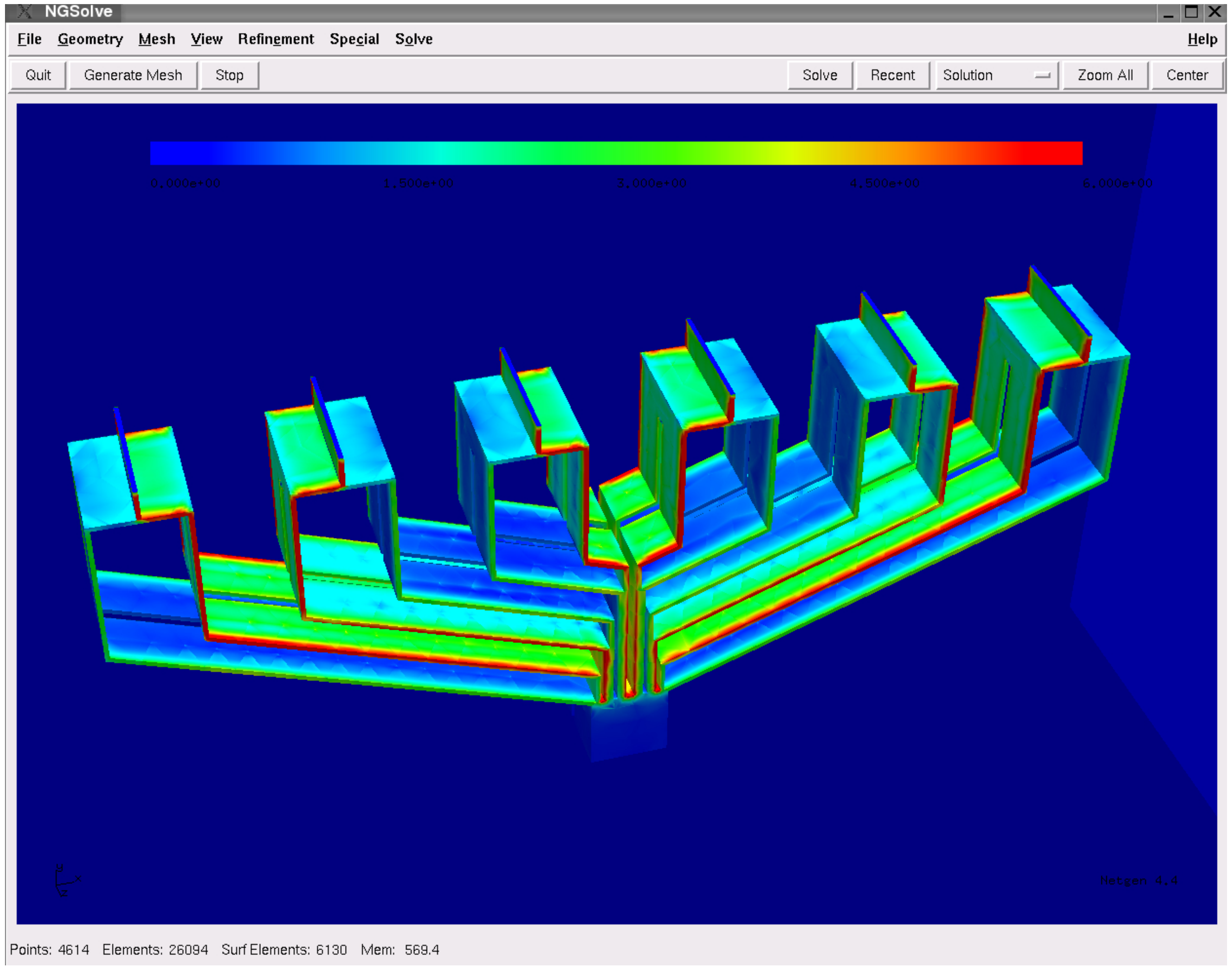

Full basis for $p = 3$ in conductor, reduced basis for $p = 3$ in air
450k complex unknowns, 20 min on P4 Centrino, 1600MHz

Fast p-FEM

time for computing one curved tetrahedral element matrix for $(\nabla u, \nabla v)$ (on 1.7 GHz notebook):

p	N_{tot}	N_{inner}	std. integration	fast integration	static cond.
	$\frac{(p+1)(p+2)(p+3)}{6}$	$\frac{(p-3)(p-2)(p-1)}{6}$	$O(p^9)$	$O(p^6)$	$O(p^9)$
4	35	1	0.0045	0.009	n.a.
8	165	35	0.198	0.041	0.001
16	816	455	16.86	1.158	0.556
24	2925	1771	n.a.	11.1	18.2

Fast integration is based on

- sum factorization for tets (Hex: Melenk et al, Tets: Karniadakis + Sherwin) ... $O(p^7)$
- utilizing recursive definition of 1D Jacobi polynomials .... $O(p^6)$

Fast matrix vector product

Fast matrix vector multiplication based on element level:

1. Given element coefficient vector u^T, compute $\sum_i u_i^T \nabla \varphi_i(x)$ in integration points ... $O(p^4)$.
2. Apply geometry data (Jacobian) and coefficient ... $O(p^3)$
3. Evaluate for test-functions ($=$ Transpose (1.))... $O(p^4)$.

Times for element-matrix element-vector multiplication (for curved elements):

p	N_{tot}	N_{inner}	fast integration [s]	static cond [s]	matrix $\times$ vector [s]
	$\frac{(p+1)(p+2)(p+3)}{6}$	$\frac{(p-3)(p-2)(p-1)}{6}$	$O(p^6)$	$O(p^9)$	$O(p^4)$
4	35	1	0.009	n.a.	0.00065
8	165	35	0.041	0.001	0.00124
16	816	455	1.158	0.556	0.00971
24	2925	1771	11.1	18.2	0.02564
32	6545	4495	n.a	n.a	0.06877

non-zero matrix entries can be reduced to $O(p^3 \times p_g)$, where p_g is the order of geometry approximation [Beuchler+JS, Report Jan. 05 (triangles)]

Preconditioning for matrix-free version

We have implemented an AS preconditioner with

- explicit low energy vertex functions
- precomputed edge $\rightarrow$ face, edge $\rightarrow$ element, face $\rightarrow$ element extensions on the reference element
- precomputed Dirchlet-inverse, and edge and face Schur complements.

Available fast DD components for tensor product elements:

- Preconditioners based on spectral equivalence to weighted h-version matrices (Jensen + Korneev)
- Wavelet preconditioners for weighted h-version matrices (Beuchler+Schneider+Schwab)
- Explicit optimal extension operators from edges to quads (Beuchler + JS, 04)

Poisson problem on a crank shaft

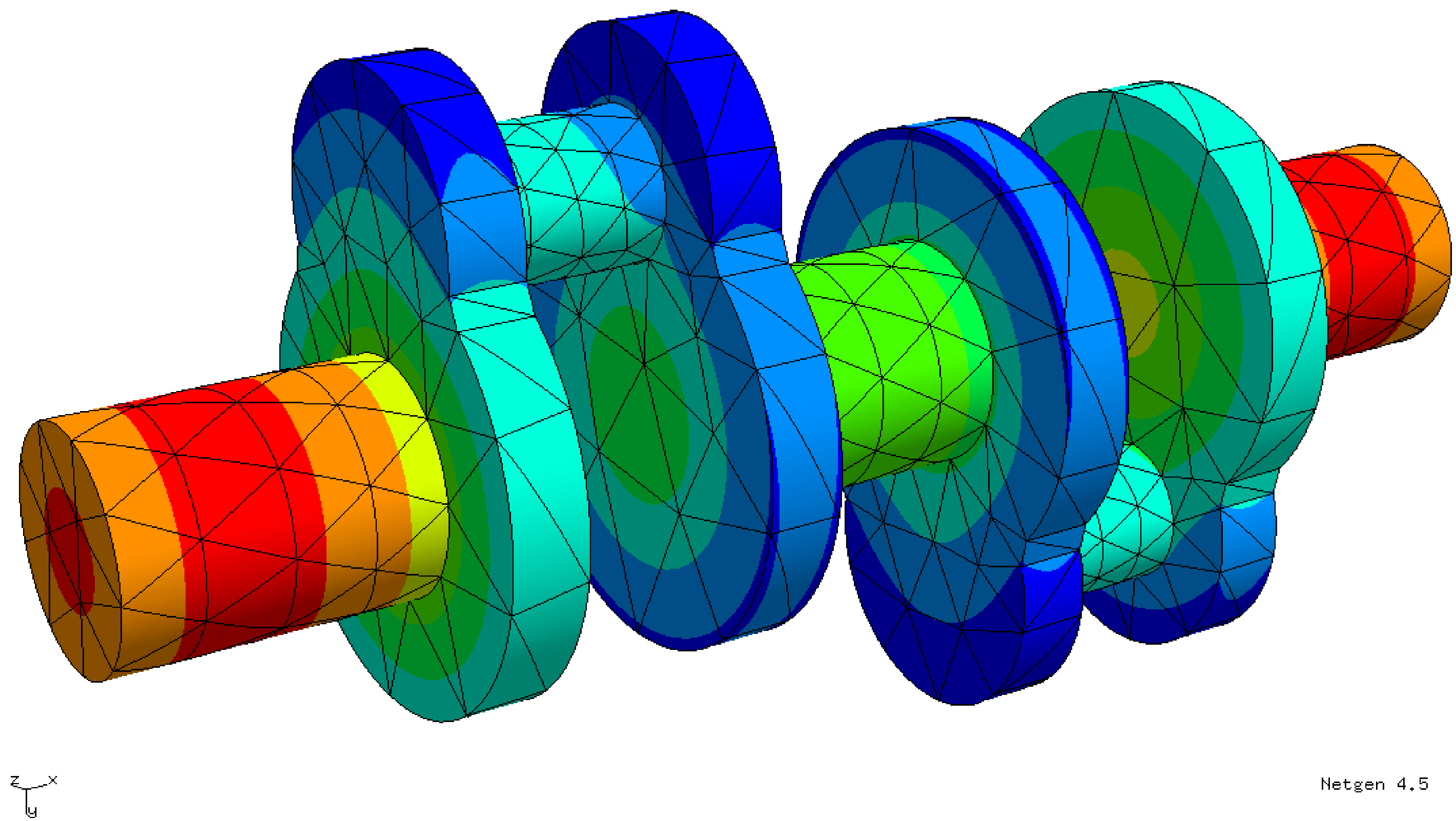

p = 12, N = 1102716, 159 iterations, total time: 20 minuts, 400 MB RAM (1.7 GHz notebook)

with flat tetrahedra, p = 15, N = 5 mio, 500 MB, 1 hour (1.7 GHz notebook)

Netgen/NGSolve Software

- **NETGEN**: An automatic tetrahedral mesh generator
  - Internal CSG based modeller
  - Geometry import from IGES/Step or STL
  - Delaunay and advancing front mesh generation algorithms
  - Arbitrary order curved elements
  - Visualization of meshes and fields
  - Open Source (LGPL), 100-150 downloads / month
- **NGSolve**: A finite element package
  - Mechanical and magnetic field problems
  - High order finite elements
  - Iterative solvers with various preconditioners
  - Adaptive mesh refinement
  - Intensively object oriented C++ (Compile time polymorphism by templates)
  - Open Source (LGPL)

Conclusion

- High order low energy basis functions for hp-FEM
- Robust two-level Schwarz analysis for $H(curl)$
- Fast p-FEM for tensor product and simplicial elements

Ongoing work:

- General implementation of matrix-free hp-FEM
- Utilize sparse element matrix on reference element for preconditioning
- Go to a big parallel computer